Investigating the Molecular Mechanisms of Action of Lenalidomide and Other Immunomodulatory Derivatives

TABLE OF CONTENTS

1 ABSTRACT

Background. Thalidomide was first released as a sedative and anti-emetic by a German pharmaceutical company in the 1950s. After its withdrawal from the market due to severe teratogenicity, thalidomide and its novel iMiD analogs were repurposed decades later for a variety of new clinical indications, including the treatment of erythema nodosum leprosum, multiple myeloma, and del(5q)-MDS. Recent work has demonstrated that iMiDs act by modulating the substrate specificity of the CRBN-CRL4 E3 ubiquitin ligase. Selective degradation of IKZF1/IKZF3 and CK1α by this complex in the presence of iMiDs leads to therapeutic activity against multiple myeloma and del(5q)-MDS, respectively. In spite of these advances, our molecular understanding of the pleiotropic effects of iMiDs remains limited. Here, we address two distinct aspects of iMiD biology that warrant further investigation: (1) substrate recognition by the iMiD-CRBN complex via degron motifs and (2) the molecular mechanism of iMiD-induced TNF-α inhibition.

Methods. Characterization of iMiD-sensitive degron motifs was performed using a flow cytometry-based fluorescent reporter assay. In brief, HEK293T cells were transfected with GFP-fusion constructs expressing wild-type and mutant degrons of IKZF3 and ZFP91. Substrate degradation in the presence of iMiD treatment was assessed by quantifying GFP reporter expression via flow cytometry. Comparison of a Drug:DMSO GFP ratio between wild-type and mutant degrons was used to determine the effects of single amino acid substitutions on iMiD-induced substrate degradation.

The mechanism of TNF-α inhibition by iMiDs was investigated by generating CRISPR/Cas9-mediated single cell knockout clones in the pro-monocytic U937 cell line. Targeted genes were components of the CRBN-CRL4 complex and its associated substrates

including CRBN, IKZF1, IKZF3, CSNK1A1, ZFP91, ZNF692, and RNF166. Knockout clones were analyzed by deep sequencing to confirm the presence of inactivating out-of-frame indels. In parallel with non-targeting sgRNA clones, validated knockout clones were treated with PMA to induce macrophagic differentiation, subjected to iMiD treatment, and then stimulated with LPS. TNF-α levels were measured by ELISA to determine any changes resulting from genetic inactivation of candidate targets.

Results. Degron mutagenesis studies revealed the presence of critical amino acid residues located in zinc-finger domain 2 of IKZF3 including Q147, C148, G152, A153, and H164. Similarly, amino acids Q401 and G406 in zinc-finger domain 4 were identified as critical residues for the ZFP91 degron. In addition, ZFP91 was validated as a CRBN-CRL4 substrate by Western immunoblotting. Lastly, preliminary TNF-α studies performed to phenotypically characterize CRBN knockout U937 clones suggested a plausible CRBN-dependent mechanism for this iMiD effect, although the results were limited by the presence of clonal heterogeneity.

Conclusions. In this study, degron characterization via a fluorescent reporter assay led to the identification of shared amino acid motifs among CRBN-CRL4 substrates that are necessary for conferring sensitivity to iMiD-inducible degradation. Future work employing structural biology approaches would be informative in elucidating the structural determinants of novel zinc-finger substrate recognition by the iMiD-CRBN complex. On the other hand, efforts to dissect the mechanism of iMiD-induced TNF-α inhibition were not fully conclusive. Although the results suggest a plausible CRBN-dependent mechanism, our experimental model warrants further refinement to overcome the limitations encountered in the present study. As an alternative approach, an unbiased proteomics experiment conducted in a monocytic system should be considered to identify novel lineage-specific targets that may provide insight into this elusive mechanism.

2 GLOSSARY

CK1 α ……casein kinase 1A1

CRBN……cereblon

CRBN-CRL4……CUL4–RBX1–DDB1–CRBN E3 ubiquitin ligase complex

CUL4……cullin-4

DDB1……damage-specific DNA-binding protein 1

del(5q)-MDS……myelodysplastic syndrome with chromosomal 5q deletion

ELISA……enzyme-linked immunosorbent assay

ENL……erythema nodosum leprosum

FGF2……fibroblast growth factor-2

GFP……green fluorescent protein

IFN- γ ……interferon-gamma

IKZF1……Ikaros

IKZF3……Aiolos

IL-2……interleukin-2

iMiD……immunomodulatory drug

LD_{50}……median lethal dose

LPS……lipopolysaccharide

MM……multiple myeloma

NF-κB……nuclear factor kappa-B

NTG……non-targeting sgRNA

PBMC……peripheral blood mononuclear cell

RBX1……RING-box protein 1

RNF166……ring finger protein 166

TNF- α ……tumor necrosis factor-alpha

ZFP91……zinc-finger protein 91

ZNF692……zinc-finger protein 692

VEGF……vascular endothelial growth factor

3 INTRODUCTION

3.1 A TRAGIC BEGINNING

Thalidomide is the first member of a class of compounds known as immunomodulatory drugs (iMiDs) that have pleiotropic biological effects including significant anti-neoplastic and anti-inflammatory activities (Table 1) [1,2]. The history of thalidomide as a drug remains exceptionally unique because its legacy has evolved dramatically over the decades since it was first released in 1954 [3]. Introduced as a novel sedative and anti-emetic, thalidomide was initially considered a miracle drug for the treatment of morning sickness in pregnant women. In a tragic turn of events, the drug was banned within a few years due to the widespread emergence of birth defects in children born to mothers who had taken it during their pregnancies [4,5]. Several decades later, thalidomide and its analogs were repurposed as therapeutic agents for the treatment of hematologic malignancies such as multiple myeloma (MM) and del(5q)-myelodysplastic syndrome (MDS) [6,7].

The tortuous history of thalidomide begins with its development by a family-owned pharmaceutical company named Chemie Grünenthal GmbH based in Stolberg, Germany. Established in 1946, this company was the first to introduce penicillin to the German pharmaceutical market in the post-World War II era. To capitalize on its initial success in the antibiotic niche, Chemie Grünenthal instituted a rapid initiative to discover new compounds with superior anti-microbial properties. Efforts to this end resulted in the somewhat accidental synthesis of a compound named α-phthalimido-glutarimide, known more commonly as thalidomide [8,9]. Although this compound did not appear to be a promising lead as an antibiotic, the company applied for a 20-year patent and began exploring its biological properties with the intent to find a commercial use.

Preliminary testing conducted by Chemie Grünenthal excluded the possibility of commercializing thalidomide as an antibiotic, antihistamine, or anticonvulsant [9]. In spite of these initial failures, the company continued to study this compound due to a promising observation that emerged from early experimentation in animals. Studies in mice and additional species revealed that thalidomide exhibited an unusually high median lethal dose (LD_{50}), defined as the dose of a compound necessary to kill one-half of a group of test animals [10]. The presumed non-toxicity of thalidomide incentivized Chemie Grünenthal to continue its search for a clinical use of this compound. To this end, researchers compared thalidomide to existing drugs and proposed a congruity between the chemical structures of thalidomide and barbiturates. Since barbiturates exhibited known sedative properties, Chemie Grünenthal moved quickly to establish the use of thalidomide for the same clinical purpose [9].

At this juncture, the evidence supporting the use of thalidomide as a sedative in humans was tenuous at best. Thalidomide and barbiturates did not exhibit significant structural overlap, and the correlation between chemical structure and biological activity was poorly defined. More importantly, thalidomide did not demonstrate any sedative effects when it was tested by researchers in a variety of animal models including mice [9]. In spite of these questionable preclinical findings, the company continued its lucrative pursuit of commercializing thalidomide as a safe sedative. The hurried decision to advance thalidomide through to trials in humans was due in large part to its favorable toxicity profile observed in animals.

Based on early successes in clinical trials, Chemie Grünenthal released thalidomide for over-the-counter use in 1957 under the trade name Contergan and marketed it widely as a sedative and an anti-emetic for pregnant women suffering from morning sickness. Initial reports claimed that the drug was safe, effective, and non-addictive [11]. As thalidomide's popularity escalated, it was eventually distributed for sale in 46 countries under different trade names for a myriad of clinical indications such as respiratory infections (Grippex), migraines (Valgraine), and

hypertension (Tensival) [12]. However, within a few years on the market, two major toxicities of thalidomide emerged that had not appeared in Chemie Grünenthal cursory testing before the drug's release. First, beginning in 1960, physicians began to report that many patients, especially the elderly, suffered from peripheral neuropathy secondary to chronic thalidomide use [13]. Furthermore, in 1961, a number of concerning reports claimed that women who had taken thalidomide during pregnancy were at a higher risk of giving birth to children with serious congenital malformations [4,5].

The discovery of thalidomide's teratogenic effects occurred through the concurrent observations of two physicians working in different countries around the same time: pediatrician Widukind Lenz in Germany and obstetrician William McBride in Australia [4,5]. Both physicians noted that children born to mothers who had taken thalidomide during their pregnancies were disproportionately affected by an atypical pattern of birth defects that included prominent limb malformations. The most common abnormality observed in these children was a shortening of proximal limb elements, also known as phocomelia [14]. Aside from various limb and digit defects, thalidomide-induced embryopathy manifested as ocular and auricular abnormalities, facial nevus, renal malformations, and congenital heart disease [15].

In the face of growing evidence demonstrating thalidomide's teratogenicity, Chemie Grünenthal withdrew the drug from the market in late 1961. This withdrawal was long overdue, as approximately 10,000 children across the world were estimated to have already been impacted by thalidomide's teratogenic effects [16]. In the the midst of this tragedy, a small piece of good news came from the United States. A new medical officer at the Food and Drug Administration (FDA) named Frances Kelsey was assigned to evaluate licensing applications for the sale of thalidomide in America. Given the troubling reports coming from Europe, Dr. Kelsey rejected the approval of thalidomide on multiple occasions and raised significant concerns about the drug's toxicity profile [17]. Indeed, through her uncompromising vigilance, Dr. Kelsey is

credited with preventing a tragic epidemic of birth deformities that may have become one of the most damaging pharmaceutical disasters in American history.

3.2 THALIDOMIDE: THE COMEBACK DRUG

With a legacy tarnished by teratogenicity, thalidomide was destined for lasting notoriety among the darkest annals of modern pharmaceutical science. Indeed, thalidomide retained its damaged reputation for many years until new research efforts spawned its revival as a therapeutic agent for previously unidentified clinical indications. The first successful attempt to repurpose thalidomide originated from the work of an Israeli dermatologist named Jacob Sheskin. Dr. Sheskin treated patients suffering from an inflammatory complication of leprosy called erythema nodosum leprosum (ENL), also known as Hansen's disease. This condition presents with painful red nodules all over the body and may be accompanied by systemic symptoms of fever, malaise, weight loss, and joint pain [18]. In order to provide relief to his patients suffering from this condition, Dr. Sheskin offered them thalidomide for its sedative properties. Unexpectedly, he observed significant improvement in the skin lesions of his patients with ENL who had been given the drug for sedation [19,20]. Based on these initial findings, a clinical trial sponsored by the World Health Organization reported in 1971 that thalidomide was superior to acetylsalicylic acid as a treatment for the cutaneous manifestations of ENL in male patients with leprosy [21]. Currently, the treatment of ENL remains one of the few FDA-approved indications of thalidomide [22].

Two decades later, interest in thalidomide resurfaced in the midst of the AIDS epidemic as a potential treatment for recurrent aphthous ulcers. Aphthous ulcers are painful oral lesions that often become a persistent and debilitating complication in the setting of HIV infection. In severe cases, the pain associated with these ulcers disrupts normal eating patterns and contributes to the wasting syndrome associated with HIV/AIDS [23]. Thalidomide was considered a promising

candidate for the treatment of this condition based on previous reports that the drug could inhibit the production of tumor necrosis factor-alpha (TNF-α), a pro-inflammatory cytokine found at elevated levels in HIV-positive patients [24,25]. A clinical trial sponsored by the National Institute of Allergy and Infectious Disease revealed that thalidomide increased complete healing of aphthous ulcers by 48%, as compared to placebo [26]. These new data prompted the FDA to give thalidomide a second look, but many HIV/AIDS patients were not willing to wait for the completion of a lengthy approval process and instead sought to acquire the drug through underground sources. With the advent of so-called "buyers' clubs," patients could purchase thalidomide and other experimental agents smuggled into the United States from the South American black market. The rising popularity of such buyers' clubs compelled the FDA to reconsider its stringent regulations on the clinical use of thalidomide across the nation [27].

In the meanwhile, a previously uncharacterized effect of thalidomide was being studied in the laboratory of esteemed vascular biologist Judah Folkman. Experimental evidence from Dr. Folkman's group indicated that thalidomide exerts an inhibitory effect on angiogenesis through a mechanism independent of the drug's immunomodulatory activity. Specifically, in a 1994 report, this group found that corneal neovascularization secondary to VEGF or FGF2 induction in rabbits was inhibited by the oral administration of thalidomide [28]. Furthermore, combination therapy of thalidomide and an anti-inflammatory agent named sulindac resulted in significant inhibition of V2 carcinoma growth in rabbits [28]. These results were intriguing in the context of Dr. Folkman's novel thesis that the growth of cancerous tumors is intrinsically dependent on the formation of new blood vessels. With this thesis in mind, the discovery of thalidomide's anti-angiogenic properties laid the foundation for its consideration as a potential anticancer agent in the years to come [3].

Thalidomide's first foray into the clinical world as a cancer treatment occurred under serendipitous circumstances at the University of Arkansas for Medical Sciences (UAMS) in late

1997. A Manhattan cardiologist named Ira Wolmer was receiving care at this institution for end-stage multiple myeloma, a deadly cancer of the plasma cell. At the age of 37, he had already failed three bone marrow transplants and an experimental vaccine [29]. Desperately seeking a cure for her husband, Beth Wolmer contacted researchers across the nation and eventually was put in touch with Dr. Judah Folkman to discuss his work on thalidomide's anti-angiogenic effects in cancer. Based on this conversation, Mrs. Wolmer approached her husband's attending physician Dr. Bart Barlogie with an unusual proposition: she requested that her husband receive thalidomide as an experimental agent to treat his terminal myeloma. Initially uncertain about pursuing this unconventional therapeutic approach, Dr. Barlogie consulted with Dr. Folkman and ultimately agreed to Mrs. Wolmer's request. The ensuing coordination of efforts between the FDA, the institutional review board at UAMS, and a pharmaceutical company named Celgene led to a rapid "compassionate use" approval of thalidomide so that it could be administered to Dr. Wolmer and another myeloma patient receiving care at this institute [30].

Unfortunately, Dr. Wolmer's disease failed to respond to the drug and he passed away a few months later in March 1998. Despite this tragic outcome, promising results emerged from the second patient who had received an experimental regimen of thalidomide along with Dr. Wolmer. This patient's myeloma exhibited a dramatic response to thalidomide treatment that culminated in near-complete remission of the disease [30]. The positive results from this patient and others who were eventually treated with the drug on a compassionate use basis led to the design of a Phase 2 study to evaluate thalidomide as a single agent in refractory MM [6]. Approximately one-third of patients in this study exhibited a favorable response to the drug, as quantified by a reduction in serum/urine paraprotein levels. The success of this trial prompted the design of large-scale Phase 3 studies to determine the efficacy of thalidomide in combination with other anti-myeloma agents such as corticosteroids, chemotherapeutic drugs, and the newer proteasome inhibitors. Several combinations of thalidomide with other agents were reported to

have a synergistic effect against MM [31-33]. In May 2006, the FDA approved thalidomide for combination therapy with dexamethasone in newly diagnosed MM patients [34]. Along with bortezomib, thalidomide became one of the first new drugs approved for this disease in over a quarter-century.

3.3 Development of Thalidomide Analogs

The emergence of new clinical indications for thalidomide stimulated the search for analogs that simultaneously exhibited enhanced therapeutic efficacy along with decreased toxicity. Celgene Corporation, a pharmaceutical company based in Summit, New Jersey, led efforts in the United States to commercialize thalidomide and develop novel derivatives once interest in the drug had been revived in the 1990s. The company first marketed thalidomide under the trade name Thalomid as a treatment for cutaneous manifestations of ENL in 1998 and later as a treatment for MM after receiving FDA approval in 2006 [22,34]. Although the resurgence of interest in the drug was welcomed with much excitement, it was clear that thalidomide had a number of flaws that could not be ignored. Certainly, the teratogenic and neuropathic effects of thalidomide were major toxicities that had been identified several decades ago following the drug's initial release. More recent testing of thalidomide revealed additional adverse reactions such as rashes, somnolence, constipation, neutropenia, thrombocytopenia, and venous thromboembolism [35]. As thalidomide made its return to the clinic, Celgene established an initiative to develop structural analogs of the drug that maximized therapeutic activity while decreasing undesirable side effects and improving its overall safety profile.

The first compound synthesized by Celgene that showed promise as a thalidomide analog was CC-5013, which later became known as lenalidomide (Figure 1a). The structure of lenalidomide is the same as thalidomide except for the presence of an amino-substitution and

the absence of a carbonyl on the phthalimide moiety. In preclinical studies, it was observed that the potency of lenalidomide was several orders of magnitude higher than thalidomide in stimulating T cell proliferation, increasing IL-2 and IFN-γ production, and decreasing LPS-stimulated TNF-α secretion by peripheral blood mononuclear cells (PBMCs) [36]. Compared to thalidomide's IC_{50} of 194 μM, lenalidomide was nearly 2,000 times more potent as an inhibitor of TNF-α secretion with an IC_{50} of 100 nM [37]. Furthermore, lenalidomide had substantially increased potency against the growth of MM cells when compared to thalidomide *in vitro*. In particular, lenalidomide had improved anti-myeloma activity against tumor cells obtained from MM patients who failed to respond to conventional therapies, suggesting that the compound could be used to overcome resistance to existing agents [38].

In a dose-escalating Phase 1 study, lenalidomide was shown to be well-tolerated with no major adverse reactions aside from drug-induced neutropenia [39]. The absence of reported somnolence, constipation, or peripheral neuropathy suggested that lenalidomide could circumvent some of the common toxicities associated with thalidomide use. Subsequent Phase 2 and 3 studies demonstrated the efficacy of lenalidomide against relapsed MM in patients who had previously received at least one anti-myeloma therapy (including thalidomide) [40,41]. Specifically, lenalidomide plus dexamethasone in comparison to dexamethasone alone was shown to significantly extend the time to disease progression (median, 11.1 months vs 4.7 months) as well as to improve overall survival [41]. These results prompted the FDA to approve lenalidomide under the trade name Revlimid in combination with dexamethasone for the treatment of relapsed MM in June 2006 [42]. In June 2015, the FDA updated this indication to include newly diagnosed MM based on clinical evidence that using lenalidomide plus dexamethasone as a first-line treatment significantly improves progression-free survival [43,44].

In addition to MM, lenalidomide was also tested as a therapy for myelodysplastic syndrome (MDS), a heterogeneous group of premalignant disorders characterized by ineffective hematopoiesis [45]. Patients with MDS often suffer from refractory anemia resulting from the deficient production of red blood cells. It has been shown previously that thalidomide leads to hematologic improvement and transfusion independence in some patients with MDS-associated refractory anemia [46]. Given its enhanced potency and reduced toxicity, lenalidomide was tested for the same indication in a preliminary trial consisting of MDS patients with transfusion-dependent or symptomatic anemia with no response to erythropoietin [47]. The results of this study were striking: 10 out of 12 patients with a 5q31.1 chromosomal deletion became transfusion-independent and achieved a partial or complete cytogenetic remission of their disease using lenalidomide. On the other hand, only 14 out of 31 patients with other karyotypes who received lenalidomide treatment became transfusion-independent, and even fewer achieved cytogenetic remission [47]. Follow-up Phase 2 and 3 studies confirmed on a larger scale that MDS with 5q deletion exhibited a distinct sensitivity to lenalidomide treatment [48-50]. One of these studies demonstrated that 76% of patients with del(5q)-MDS receiving lenalidomide had a significantly decreased dependence on transfusions, and 73% of the same cohort achieved partial or complete cytogenetic resolution of their disease [7]. Historically, a clinical response of this magnitude was unprecedented in the treatment of MDS. On the basis of these promising reports, in December 2005, the FDA approved lenalidomide for the treatment of transfusion-dependent anemia in the setting of low-risk MDS with 5q deletion [42].

Continuing their efforts to develop additional thalidomide analogs with superior clinical properties, Celgene synthesized a second compound named CC-4047 that later became known as pomalidomide. Pomalidomide consists of a glutarimide ring attached to a phthalimide moiety like its precursors, but it is distinguished by the presence of both an amino and a carbonyl substitution on the phthalimide moiety (Figure 1a). In preclinical studies, pomalidomide

demonstrated highly potent immunomodulatory activity, as evident by a 15,000-fold increase in the inhibition of TNF-α secretion by PBMCs when compared to thalidomide [37]. Moreover, in contrast to lenalidomide, pomalidomide was shown to be safe for use in patients with renal impairment. Due to significant hepatic metabolism, the unchanged renal excretion of pomalidomide is 2% compared to 82% for lenalidomide [51]. In spite of its remarkable potency and desirable metabolic properties, pomalidomide as a monotherapy for relapsed and/or refractory MM exhibited limited efficacy in a Phase 1 trial [52]. However, the combination of pomalidomide with low-dose dexamethasone achieved therapeutic synergy in patients with advanced MM who previously failed treatment with lenalidomide and/or bortezomib in follow-up studies [53,54]. A Phase 3 trial comparing pomalidomide plus low-dose dexamethasone to high-dose dexamethasone alone found that the former regimen significantly improved progression-free survival as well as overall survival in relapsed and refractory MM [55]. Given the dearth of effective therapies to treat MM in its most advanced forms, pomalidomide offered the potential to address an important unmet clinical need. Thus, in February 2013, the FDA approved pomalidomide under the trade name Pomalyst as a treatment for relapsed and refractory MM in patients who have failed two prior therapies (including lenalidomide and bortezomib) and exhibited disease progression in less than 60 days following their last treatment [56].

3.4 iMiD Mechanism of Action

iMiDs represent a unique class of pharmacological agents because their use as therapies in the clinic took place far in advance of a precise elucidation of their underlying molecular mechanisms. The resurgence of thalidomide and its analogs to treat hematologic malignancies raised a perplexing question that researchers had attempted to answer for over two decades: how are the teratogenic effects of iMiDs intertwined at a molecular level with their anti-

inflammatory and anti-myeloma properties? Early hypotheses regarding iMiD mechanisms of action proposed a complex interaction among drug-induced effects on MM cells, the tumor microenvironment, and the host's immune system. In particular, the anti-myeloma activity of iMiDs was thought to be mediated through the induction of apoptosis and growth arrest in MM cells as well as the inhibition of angiogenesis [28,38,57]. In addition, iMiDs were reported to block the adhesion of MM cells to bone marrow stromal cells, thereby leading to reduced IL-6 and VEGF secretion [58]. Finally, both the inhibition of pro-myeloma cytokine pathways involving TNF-α as well as the IL-2/IFN-γ-mediated activation of host T and natural killer cell cytotoxicity were thought to contribute to the therapeutic activity of iMiDs against MM [38,59]. Although these initial mechanisms were plausible in theory, none of them provided the necessary evidence to support a precise model for understanding pleiotropic iMiD biology.

The first major development in elucidating the molecular mechanisms of iMiD action occurred with the discovery that these drugs bind to cereblon (CRBN), the protein encoded by a gene associated with autosomal recessive mental retardation [60]. In a 2010 study, Ito *et. al.* performed affinity purification of HeLa cell extracts with thalidomide-conjugated beads and found that the drug binds directly to CRBN, which serves a substrate receptor for the previously uncharacterized CRBN-CRL4 E3 ubiquitin ligase complex [61]. The authors of this study claimed that the teratogenicity of thalidomide is mediated by its inhibition of CRBN *in vivo*. Thalidomide treatment of zebrafish embryos resulted in pectoral fin malformations, and this effect was reproduced by injecting embryos with an antisense zCRBN morpholinos oligonucleotide. Interestingly, the teratogenic effects of thalidomide treatment were blocked in zebrafish embryos overexpressing functional CRBN mutants that were defective for drug binding [61]. Ito *et. al*. argued that thalidomide-induced CRBN inhibition leads to teratogenicity by disrupting ubiquitin-mediated degradation of downstream factors involved in the normal regulation of developmental pathways. Although it was later discovered that iMiDs do not in fact inhibit E3 ubiquitin ligase

activity, the identification of CRBN as a molecular target of iMiDs provided the foundation for future investigations in the field.

The work that ultimately revealed the complete mechanism of iMiD activity in multiple myeloma was performed concurrently in laboratories led by two leading investigators affiliated with Harvard Medical School: Dr. William Kaelin of the Dana-Farber Cancer Institute and Dr. Benjamin Ebert of Brigham and Women's Hospital. Using complementary approaches, both groups determined that iMiDs bind to CRBN and modulate the substrate specificity of the CRBN-CRL4 E3 ubiquitin ligase to enhance selective degradation of Ikaros (IKZF1) and Aiolos (IKZF3) (Figure 1b) [62,63]. IKZF1 and IKZF3 are part of the Ikaros family of zinc finger transcription factors known to play an important role in mediating B cell development [64,65]. Dr. Kaelin's group arrived at this finding by using a dual luciferase reporter screen with a plasmid library of 15,483 open reading frames to measure protein level changes in the presence of lenalidomide treatment. The results of this screen indicated that lenalidomide caused selective degradation of IKZF1 and IKZF3 without affecting other members of the Ikaros family (e.g. IKZF2, IKZF4, and IKZF5). This finding was validated in MM.1S, KMS34, and L363 myeloma cell lines, which all exhibited impaired proliferation corresponding with IKZF1/IKZF3 degradation in the presence of lenalidomide treatment [62].

In parallel, Dr. Ebert's group produced a similar finding by employing a proteomics approach to quantify global changes in protein and ubiquitin levels in the presence of iMiD treatment. Specifically, SILAC (stable isotope labeling of amino acids in cell culture)-based quantitative mass spectrometry was used to analyze the proteome and ubiquitome of MM.1S myeloma cells treated with lenalidomide. Analysis of changes in protein abundance revealed significant degradation of IKZF1 and IKZF3 in lenalidomide-treated MM.1S cells [63]. These findings were validated in MM.1S cells and patient samples by demonstrating a lenalidomide-induced decrease in endogenous IKZF1/IKZF3 protein expression with no change in mRNA

levels. Furthermore, co-immunoprecipitation and *in vitro* ubiquitination studies revealed that lenalidomide promoted binding of IKZF1 and IKZF3 to the CRBN substrate receptor and subsequently increased ubiquitination and degradation of these substrates [63]. Finally, shRNA-induced knockdown of IKZF1 and IKZF3 led to growth inhibition of lenalidomide-sensitive myeloma cell lines (e.g. MM.1S, U266, NCI-H929) with no effect on lenalidomide-insensitive cells (e.g. Jurkat, Hel, and K562). Overexpression of IKZF3 in MM.1S cells generated relative resistance to the effects of lenalidomide, thereby suggesting that the therapeutic action of iMiDs is directly related to their ability to deplete IKZF1 and IKZF3 levels in myeloma cells [63]. Taken together, the findings from the laboratories of Dr. Kaelin and Dr. Ebert led to a paradigm-shifting discovery about mechanisms of pharmacological activity: for the first time, a drug was found to act by altering the specificity of an E3 ubiquitin ligase in order to target individual substrates for selective proteasomal degradation.

Following this breakthrough discovery, Dr. Ebert's laboratory shifted its focus to investigating the mechanism of lenalidomide action in del(5q)-MDS. Since MDS is a disease of the myeloid lineage, it was unlikely that degradation of the lymphoid transcription factors IKZF1 and IKZF3 could explain the activity of iMiDs in this therapeutic context. SILAC-based quantitative mass spectrometry was used to analyze changes in the proteome and ubiquitome of del(5q) myeloid KG-1 cells treated with lenalidomide. This analysis revealed increased ubiquitination and decreased protein abundance of a novel CRBN-CRL4 substrate named casein kinase 1A1 (CK1α), a protein encoded by the CSNK1A1 gene located within the common deleted region of del(5q)-MDS [66]. CK1α is a multifunctional serine/threonine kinase that has been reported to negatively regulate Wnt signaling and to inhibit p53 via MDMX/MDM2 [67-69]. Importantly, previous studies have linked CK1α to the biology of del(5q)-MDS and acute myeloid leukemia [70,71].

Given that CK1 α is expressed at 50% lower levels in del(5q)-MDS cells, Dr. Ebert's group hypothesized that the state of CK1 α haploinsufficiency conferred a therapeutic window for the efficacy of lenalidomide in this disease. Efforts to test this hypothesis began with demonstrating degradation of endogenous CK1 α protein with no effect on mRNA levels in multiple cell lines treated with lenalidomide. In addition, co-immunoprecipitation and *in vitro* ubiquitination studies revealed that lenalidomide increased binding of CK1 α to CRBN, thereby leading to increased ubiquitination and degradation of this substrate [66]. Finally, CSNK1A1 was ectopically overexpressed in CD34+ cells obtained from del(5q)-MDS patients, normal karyotype MDS patients, and healthy donors. CSNK1A1 overexpression led to an isolated decrease in the lenalidomide sensitivity of del(5q)-MDS cells with no effect on the others, suggesting that the depletion of CK1 α levels is essential for mediating the clinical response of del(5q)-MDS to lenalidomide [66].

While thalidomide, lenalidomide, and pomalidomide all exhibit therapeutic activity in multiple myeloma via IKZF1/IKZF3 degradation, only lenalidomide has been shown to be effective in treating del(5q)-MDS. In this context, Dr. Ebert's group sought to determine whether all members of the iMiD family induce degradation of the same CRBN-CRL4 E3 ubiquitin ligase substrates. Using a tandem mass tag (TMT) quantitative proteomics approach in the MDS-L cell line, protein abundance levels were compared between samples treated with lenalidomide versus CC-122, a novel CRBN-binding drug currently being studied in clinical trials. Lenalidomide treatment led to significant degradation of IKZF1 and CK1 α as expected, but CC-122 treatment led to even more potent degradation of IKZF1 with no effect on CK1 α [66]. Although all iMiDs induced degradation of IKZF1, validation by Western blotting confirmed that lenalidomide was the only iMiD derivative that could efficiently degrade CK1 α. No degradation of CK1 α was observed upon treatment with CC-122 and thalidomide, while pomalidomide had

a very minimal effect [66]. These results indicate that the substrate specificities of iMiDs may be regulated by structural factors that allow each drug to target a unique set of proteins for degradation by the CRBN-CRL4 E3 ubiquitin ligase complex.

Detailed insight into the conformational aspects of iMiD-substrate interactions was obtained through generation of 3-D crystal structures for the CRBN-DDB1-thalidomide and CRBN-DDB1-lenalidomide complexes as well as the recent CRBN-DDB1-lenalidomide-CK1 α crystal structure solved by Petzold *et. al* [72-74]. With a CRBN-DDB1 crystal structure bound to both drug and substrate, Petzold *et. al.* demonstrated that the interaction between CK1 α and CRBN in the presence of lenalidomide results in a shift of C3 on its phthalimide ring to the carbonyl group of a Glu377 residue located in the CRBN backbone [74]. Since the phthalimide moieties of thalidomide and pomalidomide contain a C3 carbonyl group absent in lenalidomide, it is likely that steric clash disfavors the recruitment of CK1 α to the CRBN-CRL4 ligase by these two drugs. This finding offered the last piece of evidence needed to formulate a precise mechanistic explanation for the selective activity of lenalidomide over other iMiDs in del(5q)-MDS. With the elucidation of this mechanism, lenalidomide became the first pharmaceutical success based on a decades-old concept that heterozygous gene deletions could be exploited as therapeutic vulnerabilities against cancer [75,76].

The investigation of lenalidomide activity in del(5q)-MDS by Dr. Ebert's laboratory unexpectedly led to the answer for a tangential question of historical importance regarding mechanisms of iMiD activity: namely, what is the molecular basis for the differential species-specific effects exerted by this class of therapeutic agents? One of the key factors that contributed to the thalidomide disaster of the late 1950s was the complete absence of teratogenicity observed in rodent models during preclinical drug studies. Ironically, the intrinsic lack of murine response to thalidomide prompted early investigators to deem the drug exceptionally safe as a result of the high LD_{50} values observed in this species [10].

To address the incongruity between mouse and human responses to iMiDs, Krönke *et. al.* first overexpressed human CRBN in murine Ba/F3 cells and observed degradation of CK1α in the presence of lenalidomide that was not seen upon overexpression of mouse Crbn in the same system [66]. Next, human/mouse CRBN chimeric proteins were overexpressed in Ba/F3 cells and assessed for their ability to cause lenalidomide-induced CK1α degradation in order to localize the iMiD-binding region of CRBN. This analysis revealed that lenalidomide sensitivity was driven by the C-terminal half of CRBN, a region that has only five non-conserved residues between mice and humans. When these five residues in human CRBN were modified to their counterparts in mouse Crbn, only the V387I mutation resulted in a disruption of response to lenalidomide, as measured by a loss of CK1α degradation. On the other hand, conferral of lenalidomide sensitivity was observed via drug-induced degradation of CK1α, IKZF1 and IKZF3 when a Crbn(I391V) point mutant was generated to modify the key residue in mouse Crbn to its counterpart in human CRBN [66].

Finally, Krönke *et. al.* employed a structural biology approach based on recently solved crystal structures of various CRBN-DDB1-iMiD complexes to model the conformational effects of CRBN amino acid substitutions. In particular, the authors proposed that the lack of murine sensitivity to iMiDs is caused by the presence of a bulky isoleucine sidechain in murine Crbn (position 391) versus valine in human CRBN (position 387). This substitution leads to steric clash and the obstruction of hydrogen bonds essential for substrate recruitment to the CRBN-CRL4 ubiquitin ligase complex [66]. In aggregate, the data suggest that a single amino acid difference between mouse and human CRBN is responsible for the disparate iMiD sensitivities exhibited by these two species. Indeed, by describing the species-specific effects of iMiDs at a molecular level, this model offers mechanistic insight into the tragic discrepancy between mice and humans that led to the use of thalidomide in pregnant women in spite of its severe teratogenicity.

3.5 PURPOSE OF INQUIRY

The purpose of the present inquiry can be divided into two interrelated aims, as follows:

1) The first objective of this study was to characterize the degron sequence in iMiD-targeted substrates of the CRBN-CRL4 E3 ubiquitin ligase complex. By definition, the degron is the smallest element within a protein that is both necessary and sufficient to direct signals for degradation by its cognate ubiquitin ligase [77]. Previously, Krönke *et. al.* tested a series of deletion mutants and identified a 59-amino acid degron sequence present in zinc finger 2 domain of IKZF3 that is responsible for mediating its sensitivity to lenalidomide-induced degradation [63]. As an extension of this work, the present study seeks to further define the degron sequence of iMiD-targeted substrates with a resolution at the level of single amino acid residues. By generating point mutants and assessing iMiD-induced degradation using a fluorescent reporter assay, we conducted a detailed examination of the degron sequences present in both validated and novel CRBN-CRL4 E3 ubiquitin ligase substrates including IKZF3 and ZFP91. The rationale to perform these studies was to gain additional insight into the molecular mechanisms of iMiD activity through an understanding of the structural determinants that mediate target recognition by the iMiD-CRBN complex.

2) The second objective of this study was to determine which substrate(s), if any, of the CRBN-CRL4 E3 ubiquitin ligase complex mediate the immunomodulatory properties of iMiDs, with a particular emphasis on the inhibitory TNF-α effect of these drugs. For more than two decades, iMiDs have been reported to downregulate secretion of TNF-α by monocytes. In particular, thalidomide has been shown to potently inhibit TNF-α in LPS-stimulated monocytes via a mechanism dependent on increased mRNA degradation [78,79]. Furthermore, since the newer iMiD analogs were developed to exhibit enhanced

immunomodulatory properties, it has been reported that lenalidomide and pomalidomide inhibit TNF-α secretion even more strongly than their parent compound, as evident by respective IC_{50} values 2,000 and 15,000 times more potent than that of thalidomide [37]. Although the effect of TNF-α blockade by iMiDs has been reported for several years, the underlying molecular mechanism remains unclear at present. By generating CRISPR/Cas9 single-cell clones in a monocytic cell line, we sought to genetically inactivate isolated components of the CRBN-CRL4 E3 ubiquitin ligase complex in order to determine whether knocking out any of these factors affected TNF-α levels in the presence and absence of iMiD treatment. The rationale behind this part of the present inquiry was to establish a molecular mechanism that could explain iMiD-induced TNF-α downregulation, with an eye toward optimizing the immunomodulatory properties of novel iMiD derivatives for use in the treatment of autoimmune diseases and disorders of immune dysregulation.

4 MATERIALS AND METHODS

4.1 MUTANT DEGRON ANALYSIS VIA A FLUORESCENT REPORTER ASSAY

IKZF3 degron mutagenesis and analysis. Plasmid expression vectors containing amino acid residues 146-168 of the IKZF3 degron sequence fused to GFP via a flexible linker were constructed and prepared by Quinlan Sievers (Figure 2a). Specifically, constructs for the wild-type sequence and the following eight point mutants of IKZF3 AA146-168 were kindly provided: Q147E, Q147N, G152A, G152S, A153G, A153V, C148A, and H164A. HEK293T cells were cultured in Dulbecco's Modification of Eagle (DMEM) medium (Thermo Fisher Scientific) with 10% fetal bovine serum (Sigma-Aldrich) and 1% penicillin-streptomycin-glutamine (Life Technologies) 37°C/5% CO_2. 2 x 10^5 HEK293T cells were transfected with 5 µg of each plasmid using the TransIT-LTI transfection reagent (Mirus Bio) according to the manufacturer's instructions. Puromycin (Life Technologies) treatment at a dose of 2 µg/mL was initiated 72 h-post transfection for a duration of 48 h to select for transfected cells. Following selection, cells were plated at a density of 2.5 x 10^4 cells/well in a 96-well tissue culture plate and dosed in triplicate with 0.1% DMSO (VWR) versus lenalidomide (Selleck Chemicals) and pomalidomide (Selleck Chemicals) at 0.1 µM, 1 µM, and 10 µM for 18 h. Drug dilutions were performed in cell culture media to ensure a final DMSO concentration of 0.1%.

Next, flow cytometry of DMSO- and drug-treated cells was performed on a FACSCanto II system (BD Biosciences) using a High-Throughput Sampler (HTS). The FITC channel was used to detect GFP reporter expression. DAPI staining, as detected by the Pacific Blue channel, was used to exclude dead cells. At least 10,000 events were recorded per well. Results obtained from flow cytometry were analyzed using FlowJo software. For each treatment condition, analysis was performed by calculating a drug/DMSO GFP+ ratio. This value was obtained by dividing the percentage of GFP+ cells in the drug-treated samples by that of the DMSO-treated controls. All

results were reported as an average of three technical replicates with error bars representing standard error of the mean.

ZFP91 degron mutagenesis and analysis. Plasmid expression vectors containing the full-length ZFP91 sequence fused to GFP via a rigid linker were constructed and prepared by Quinlan Sievers (Figure 4b). Specifically, constructs for the wild-type sequence, a zinc finger 4 domain-deletion mutant, and the following five point mutants of ZFP91 were kindly provided: Q401N, G406A, G406N, F407Y, and F407R. Cell culture, transfection/selection of HEK293T cells, drug treatments, and analysis via flow cytometry were conducted using the procedure described above.

4.2 Generation of CRISPR/Cas9 Single-Cell Knockout Clones

sgRNA design and plasmid preparation. Genes targeted for CRISPR/Cas9-mediated genome editing in this study include IKZF1, IKZF3, CSNK1A1, CRBN, ZFP91, ZNF692, and RNF166. Two high-scoring sgRNAs per target gene were designed using the Broad Institute's online sgRNA design tool, as described in Doench *et. al.* [80]. A non-targeting sgRNA (NTG) was also included as a control. DNA oligonucleotides for the selected sgRNA sequences (Table 2) were synthesized (Integrated DNA Technologies), and cloned into lentiviral CRISPR backbones pL-CRISPR.EFS.GFP or pxPR_001 (Addgene). Specifically, 5 µg of each vector backbone was digested with the BsmBI restriction enzyme (New England Biolabs) for 1 h at 55ºC, dephosphorylated for 30 min with Antarctic Phosphatase (New England Biolabs), and purified using the QIAQuick PCR Purification Kit (Qiagen) according to the manufacturer's instructions. Oligonucleotide pairs were annealed and phosphorylated with T4 PNK (New England Biolabs) using the following thermocycling conditions: 37ºC for 30 min, 95ºC for 5 min, ramp down 5º/min

until 25ºC. Dephosphorylated vector backbones and annealed/phosphorylated oligonucleotide pairs were then ligated overnight at 16ºC. OneShot TOP10 *E. coli* chemically competent cells (Thermo Fisher Scientific) were transformed with each ligation, as per manufacturer's instructions. LB cultures were inoculated with single colonies from each transformation and grown at 37ºC for 18 h. Plasmid DNA was purified using a QIAPrep Spin Mini Kit (Qiagen) according to the manufacturer's instructions and screened by Sanger sequencing (Genewiz, Inc.) to select for colonies containing vector ligated with insert. OneShot Stbl3 *E. coli* chemically competent cells (Thermo Fisher Scientific) were retransformed with miniprepped DNA from positive colonies. Finally, plasmid DNA was purified for lentiviral production using the QIAPrep Plasmid Plus Midi Kit (Qiagen) according to the manufacturer's instructions.

Lentiviral production and transduction. For each construct of interest, 1 x 10^6 HEK293T cells were transfected with 5 µg of plasmid DNA, 3 µg of psPAX2 packaging vector, and 0.3 µg of VSV-G envelope vector by using TransIT-LT transfection reagent (Mirus Bio) according to the manufacturer's instructions. After 72 h, viral supernatants were harvested, filtered through a 0.45 µm syringe filter, and stored at -80 ºC until use. 2 x 10^6 U937 cells (ATCC) were transduced with 1 mL of lentivirus in a 6-well tissue culture plate in the presence of 4 µg/mL hexadimethrine bromide (Sigma-Aldrich). Transduced cells were spinfected in a benchtop centrifuge for 90 min at a speed of 500 g at 37ºC. Cells were cultured for 7 days in RPMI 1640 medium (Thermo Fisher Scientific) with 10% fetal bovine serum and 1% penicillin-streptomycin-glutamine at 37ºC/5% CO_2. During this period, cells transduced with pxPR_001 backbone-derived vectors were subjected to puromycin selection at a dose of 2 µg/mL.

Single-cell sorting. Following the completion of lentiviral Cas9-sgRNA vector transduction, U937 cells were prepared for single-cell sorting on a FACSARIAII system (BD Biosciences) operated

by the Children's Hospital of Boston/Harvard Stem Cell Institute flow cytometry core facility. Cells transduced with pL-CRISPR.EFS.GFP backbone-derived vectors were gated for viability and GFP expression. Cells transduced with pxPR_001 vectors were gated for viability (following puromycin selection). Single cells from the appropriate gate were sorted into 96-well tissue culture plates using a 70-μm nozzle tip. Three 96-well plates of single cells were sorted for each Cas9-sgRNA construct. After sorting, cells were expanded under the culture conditions described above. Viable clones were screened visually by assessing the level of confluency in the 96-well plate. Selected clones were subsequently transferred to 24-well and 12-well tissue culture plates for expansion. Upon reaching confluency in a 12-well plate, each clone was divided into two aliquots. One aliquot was frozen for storage at -80°C, and the other aliquot was used to extract genomic DNA.

Knockout clone screening via next-generation sequencing. Genomic DNA was extracted from each single-cell clone using a QIAamp 96-well DNA Blood Kit (Qiagen) according to the manufacturer's instructions. PCR primers flanking each CRISPR target site were designed to amplify the surrounding genomic region with a desired amplicon length of 200-300 base pairs Table 3). Phusion High-Fidelity PCR Master Mix with GC Buffer (New England Biolabs) was used to perform PCR amplification under standard thermocycling conditions, as described in the manufacturer's instructions. 1% agarose DNA gel electrophoresis was used to visualize PCR products and confirm successful amplification. PCR products were then purified by using a QIAquick PCR Purification Kit according to the manufacturer's instructions. Purified PCR amplicons were submitted to the MGH DNA Core Facility for next-generation Illumina sequencing. For each gene of interest, sequencing reads were aligned to reference amplicon sequences in CLC Sequence Viewer 7 to identify single-cell clones containing inactivating out-of-frame indels induced by CRISPR/Cas9.

4.3 WESTERN IMMUNOBLOTTING

CRBN-CRL4 substrate validation. KG-1 cells (ATCC) were treated for 18 h with 0.1% DMSO, 10 μM and 50 μM thalidomide (Sigma-Aldrich), 1 μM and 10 μM lenalidomide, and 1 μM and 10 μM pomalidomide. Drug dilutions in cell culture media were performed to ensure a final DMSO concentration of 0.1%. Following drug treatment, cells were washed with phosphate-buffered saline (PBS) and lysed on ice for 30 min using IP Lysis Buffer (Pierce Biotechnologies) in the presence of Halt Protease and Phosphatase Inhibitor Cocktail (Life Technologies). Following the harvest of protein lysates, total protein concentrations for each sample were measured by using a Protein BCA Assay (Pierce) according to the manufacturer's instructions. Equal amounts of protein lysates were run on Criterion Precast 4-15% Tris-HCl gels (Bio-Rad) at a constant voltage of 120 V for 1 h. Proteins were transferred to an Immobilon-P PVDF transfer membrane (Millipore) at a constant amperage of 0.60 A for 1 h. Ponceau S (Sigma-Aldrich) staining was used to confirm successful protein transfer, followed by membrane blocking with 5% non-fat dry milk (Thermo Fisher Scientific) in TBS-T for 1 h at room temperature. Membranes were incubated overnight at 4ºC with the primary antibody. For detection of ZFP91, polyclonal rabbit anti-ZFP91 antibody (Bethyl Laboratories #A303-245) was diluted 1:1000 in a solution of 5% BSA (Boston Bioproducts) in TBS-T. After 3 x 5 min washes in TBS-T, the membrane was incubated for 1 h at room temperature with an HRP-conjugated donkey anti-rabbit IgG secondary antibody (VWR # 95017-556) diluted 1:5000 in a solution of 5% non-fat dry milk in TBS-T. Staining with a HRP-conjugated mouse monoclonal antibody to ß-actin (Abcam #ab20272) served as the loading control for these experiments. Following 3 x 5 min TBS-T washes and a 1 x 5 min TBS wash, blots were treated with SuperSignal West Pico Chemiluminescent Substrate or SuperSignal West Dura Extended Duration Chemiluminescent Substrate (Pierce Biotechnologies) according

to the manufacturer's instructions and then developed on HyBlot-CL autoradiography film (Denville Scientific).

Single-cell knockout clone validation. Protein lysates were prepared from clones known to have CRISPR/Cas9-mediated inactivating out-of-frame indels by deep sequencing. Comparison to lysates prepared from non-targeting sgRNA clones served as the control. Primary antibodies used for detection of target protein expression included a polyclonal rabbit anti-CRBN antibody (Novus Biologicals #NBP191810) diluted 1:1000 in 5% BSA in TBS-T and the anti-ZFP91 antibody referenced above. The remainder of the Western immunoblotting procedure was performed under standard conditions described in the previous section.

4.4 TNF-α Enzyme-Linked-Immunosorbent Assay (ELISA)

U937 cells were seeded at a density of 5 x 10^4 cells per well in a 96-well plate and cultured under the conditions described above. 24 h after the initial seeding, cells were treated with 100 nM phorbol 12-myristate 13-acetate (PMA) (Sigma-Aldrich) to induce differentiation toward a more macrophage-like state. After 24 h of PMA treatment, culture medium was replaced without additional PMA and cells were allowed to continue differentiation for another 24 h. Cells were then dosed in triplicate with 0.1% DMSO, 1 μM and 10 μM lenalidomide, and 1 μM and 10 μM pomalidomide. 4 h after drug treatment, cells were stimulated for 16 h with 100 ng/mL lipopolysaccharide (LPS) derived from *E. coli* 0111:B4 (Santa Cruz Biotechnology). Supernatants were collected and diluted 1:5 in cell culture medium before TNF-α levels were analyzed by using the QuantiGlo Human TNF-α ELISA Kit (R & D Biosystems) according to the manufacturer's instructions. Luminescence readings were taken on a DTX880 microplate reader (Beckman Coulter) and, when possible, were normalized to cell number as determined by the

Cell-Titer Glo Cell Viability Assay (Promega). For each plate reading, a standard curve was generated using standard samples provided in the ELISA kit. All results were reported as an average of three technical replicates with error bars representing standard error of the mean.

5 RESULTS

The results presented in Sections 5.1 and 5.3 were obtained in collaboration with Quinlan Sievers. Sievers performed a screen to identify critical amino acid residues in the IKZF3 degron and designed the fluorescent reporter constructs used here to validate the results of the degron screen. After receiving these plasmids, I performed the transfections, selection, drug treatments, flow cytometry, and data analysis. In addition, the results presented in Section 5.2 validate findings from proteomics studies previously published by Krönke *et. al* [63, 66]. Finally, the results presented in Sections 5.4 and 5.5 were obtained through my independent efforts.

5.1 EFFECTS OF IKZF3 DEGRON MUTAGENESIS ON SUBSTRATE RECOGNITION BY THE IMID-CRBN COMPLEX

In order to identify critical amino acid residues within the IKZF3 degron, we generated a series of point mutants and assessed their degradation in the presence of iMiD treatment using a fluorescent reporter assay. Previously, Krönke *et. al* tested multiple IKZF3 deletion mutants and identified a lenalidomide-sensitive degron sequence of 59 amino acids (residues AA130-189) located within the protein's zinc finger 2 (ZF2) domain [63]. A graduate student in the Ebert Lab named Quinlan Sievers continued efforts to characterize the IKZF3 degron by generating a MITE-seq comprehensive saturating mutagenesis library. This library contained an array of constructs in which single mutations were made to IKZF3 AA130-189 so that all 20 amino acids were substituted at each position along the degron sequence. The library was cloned into a fluorescent reporter vector and transfected into HEK293T cells that were treated with thalidomide, lenalidomide, and pomalidomide for 20 h. Following drug treatment, the library was screened by flow cytometry to assess the effects of site-specific degron mutagenesis on IKZF3 degradation. The results of this screen allowed Sievers to narrow down the critical IKZF3 degron

sequence to residues AA146-168, a region that appeared to contain nine essential amino acids for mediating iMiD sensitivity: Q147, C148, C151, G152, A153, F155, L161, H164, and H168.

Despite offering preliminary insight into the structural composition of the IKZF3 degron motif, this screen did not provide the necessary statistical power to make valid conclusions about the effect of single amino acid substitutions on iMiD-induced substrate degradation. As a result, in the present study, we sought to statistically validate the findings of this degron screen by analyzing a series of IKZF3 degron point mutants via a fluorescent reporter assay. To this end, plasmids for the following site-specific mutants of the IKZF3 degron fused to GFP with a flexible linker were constructed and prepared by Quinlan Sievers: Q147E, Q147N, G152A, G152S, A153G, A153V, C148A, and H164A (Figure 2b). HEK293T cells were transfected with each of the provided constructs, selected with puromycin, and treated with DMSO or lenalidomide/pomalidomide (0.1, 1, and 10 μM) for 18 h. Analysis of treated samples by flow cytometry led to the calculation of a normalized Drug:DMSO GFP ratio used to assess degradation of mutant degrons compared to the wild-type degron at a given dose of lenalidomide or pomalidomide.

Our results demonstrate with statistical significance that mutating single critical residues of the IKZF3 degron sequence is sufficient to block substrate degradation in the presence of iMiD treatment (Figure 2c). Specifically, seven out of eight point mutants tested (Q147E, Q147N, G152A, G152S, A153G, C148A, and H164A) led to complete impairment of IKZF3 degradation even when treated with the highest doses of lenalidomide and pomalidomide. While it did not have a complete effect, the IKZF3 A153G mutant exhibited partial resistance to iMiD-induced degradation (Figure 2c). In aggregate, these results indicate that single amino acid residues located within the IKZF3 degron play a critical role in mediating iMiD sensitivity, thereby offering novel insight into the structural determinants of substrate recognition by the iMiD-CRBN complex.

5.2 VALIDATION OF ZFP91 AS A NOVEL CRBN-CRL4 E3 UBIQUITIN LIGASE SUBSTRATE

Next, we sought to determine whether novel substrates of the CRBN-CRL4 E3 ubiquitin ligase contained iMiD-sensitive structural motifs similar to the degron sequences characterized for known substrates such as IKZF1 and IKZF3. Previously, our group conducted SILAC-based proteomics experiments in MM.1S and KG-1 cells to identify targets whose protein abundance was significantly depleted in the presence of lenalidomide treatment [63,66]. In addition to known substrates IKZF1, IKZF3, and CK1α, the results of these experiments identified a number of proteins that may be novel targets for degradation by the iMiD-CRBN complex. In particular, three new zinc-finger proteins emerged as attractive candidates for further investigation: ZFP91, ZNF692, and RNF166 (Figure 3a).

Of these three targets, ZFP91 was selected as the focus of our initial efforts because of existing pSILAC mass spectrometry results corroborating its role as an iMiD-dependent CRL4-CRBN substrate and the presence of preliminary data investigating its potential biological function [81]. Of note, ZFP91 has been shown to positively regulate non-canonical NF-□B signaling by promoting stabilization of NIK through Lys^{63}-linked ubiquitination [82,83]. Given that the NF-□B signaling plays an important role in regulating immunity, inflammation, and carcinogenesis, the characterization of ZFP91 as a novel target could provide a molecular basis for iMiD-associated effects that have eluded a mechanistic explanation [84,85]. Specifically, iMiD-induced degradation of ZFP91 and downstream alterations in NF-□B signaling could play a role in mediating the immunomodulatory effects of these drugs, such as decreased TNF-α secretion.

Validation of ZFP91 as a novel CRBN-CRL4 substrate was performed by assessing protein degradation in the presence of iMiD treatment via Western immunoblotting. KG-1 cells were

treated for 18 h with DMSO, thalidomide (10 μM and 50 μM), lenalidomide (1 μM and 10 μM), and pomalidomide (1 μM and 10 μM). Initial attempts to detect ZFP91 with primary antibodies from Abcam (#ab30970) and Santa Cruz (#sc-102172) were unsuccessful due to technical difficulties arising from non-specific binding. Successful detection of ZFP91 was achieved with the use of a rabbit polyclonal anti-ZFP91 antibody from Bethyl Laboratories (#A303-245A). In the presence of pomalidomide (POM) at 1 μM and 10 μM, nearly complete degradation of ZFP91 was observed by Western blot (Figure 3b). In contrast, significant degradation of ZFP91 was not observed with thalidomide (THAL) and lenalidomide (LEN) treatment, further reinforcing the previously established notion that individual members of the iMiD family may exert differential substrate specificities [66].

5.3 Effects of ZFP91 Degron Mutagenesis on Substrate Recognition by the iMiD-CRBN Complex

Having validated ZFP91 as a novel CRBN-CRL4 substrate by Western immunoblotting, we focused our efforts on characterizing an iMiD-sensitive degron motif within this protein. The amino acid sequences of IKZF3 and ZFP91 were aligned in order to identify shared regions of homology. This alignment revealed that the degron sequence in the zinc finger 2 (ZF2) domain of IKZF3 aligned closely with the zinc finger 4 (ZF4) domain of ZFP91 (Figure 4a). Indeed, both regions shared a unique QCXXCG motif not found in the zinc finger domains of other proteins. Based on the amino acid sequence homology, we hypothesized that residues spanning AA400-422 served as the key degron motif for ZFP91 in a manner similar to residues AA146-168 for IKZF3.

We investigated this hypothesis by testing a series of ZFP91 point mutants using a fluorescent reporter assay similarly designed in parallel to the aforementioned assay for IKZF3 degron mutagenesis. Plasmids for the following site-specific mutants of full-length ZFP91 fused

to GFP with a rigid linker were constructed and prepared by Quinlan Sievers: Q401N, G406A, G406N, F407Y, and F407R (Figure 4b). As described above, HEK293T cells were transfected with each of the provided constructs and selected with puromycin. Following 18-h treatment with DMSO or lenalidomide/pomalidomide (0.1, 1, and 10 μM), samples were analyzed by flow cytometry in order to calculate a normalized Drug:DMSO GFP ratio. This ratio was used to measure degradation of ZFP91 point mutants in comparison to wild-type ZFP91 in the presence of iMiD treatment at multiple doses.

Our results reveal that mutating single residues in the ZFP91 ZF4 domain leads to statistically significant impairment of iMiD-induced degradation, suggesting this region serves a function analogous to that of the degron in the IKZF3 ZF2 domain. At baseline, degradation of wild-type ZFP91 in the presence of iMiD treatment was less efficient than degradation of IKZF3 AA146-168 (Figures 2c, 4c). In this assay, minimal degradation of wild-type ZFP91 was observed with lenalidomide treatment at 1 μM and 10 μM. However, greater than 50% degradation of wild-type ZFP91 was observed with pomalidomide treatment at 1 μM and 10 μM (Figure 4c), which is consistent with the results obtained via Western immunoblotting (Figure 3b). Clearly, pomalidomide-induced ZFP91 degradation was abrogated in the control ZF4-deletion mutant as well as in the Q401N, G406A, and G406N point mutants. On the other hand, the F407Y and F407R point mutants did not exhibit significant resistance to iMiD-induced degradation (Figure 4c). Of note, the F407 residue in the ZF4 domain of ZFP91 does not match the equivalent residue (A153) of the IKZF3 degron sequence (Figure 4a). Taken together, these data demonstrate that both established and novel CRBN-CRL4 substrates contain iMiD-sensitive degrons characterized by shared elements of amino acid sequence homology. Although these degron sequences share broad similarities across individual substrates, differences in single amino acids positioned at critical residues appear to significantly alter substrate recognition by the iMiD-CRBN comple

5.4 iMiD-Induced TNF-α Downregulation in U937 Monocytic Cells

The second chapter of this study focused on investigating a molecular basis for the inhibitory effect of iMiDs on TNF-α secretion. In order to approach this question, we searched for an appropriate *in vitro* system that would accurately reflect iMiD-induced effects on monocytic cytokine secretion while permitting genetic manipulation to conduct mechanistic studies. Pilot experiments were performed in order to determine which monocytic cell line(s) exhibited maximal sensitivity to iMiD treatment, as measured by TNF-α downregulation on ELISA. Among the cell lines tested (including THP-1 and HL-60), the pro-monocytic U937 cell line emerged as the most sensitive system for studying the effects of iMiDs on TNF-α secretion [86]. When treated with lenalidomide and pomalidomide at doses of 1 μM and 10 μM, PMA-differentiated U937 cells exhibited approximately a 30-40% decrease in TNF-α secretion (Figure 5). The magnitude of this effect is consistent with previous studies that have reported ~40% inhibition of TNF-α production using primary human monocytes [78].

5.5 Effects of CRISPR/Cas9-Mediated CRBN Inactivation on iMiD-Induced TNF-α Downregulation

After selecting a model system for the investigation of iMiD-induced TNF-α downregulation, we moved forward with generating single-cell knockout clones via CRISPR/Cas9 genome editing in the U937 cell line. As described above, single-cell knockout clones were generated using two sgRNAs predicted to efficiently target each of the following genes: CRBN, IKZF1, IKZF3, CSNK1A1, ZFP91, ZNF692, and RNF166. Our first study using these knockout clones aimed to investigate whether iMiDs downregulate monocytic TNF-α secretion through a mechanism dependent on CRBN. For this initial assay, we selected four

U937 single-cell knockout clones generated from CRBN sgRNA #2 (Table 2) that were shown to have triallelic out-of-frame indels in Exon 5 by deep sequencing. Clone 2.5 had two 1-bp deletions and one 17-bp deletion. Clone 2.7 had one 1-bp deletion, one 1-bp insertion, and one 2-bp insertion. Clone 2.10 had one 1-bp insertion, one 1-bp deletion, and one 17-bp deletion. Clone 2.12 had one 1-bp insertion, one 2-bp deletion, and one 25-bp deletion. In addition, the four selected clones were shown to be CRBN knockouts at the protein level via Western immunoblotting (Figure 6a).

Following validation of the selected knockout clones, we investigated the effects of CRISPR/Cas9-induced CRBN inactivation on TNF-α downregulation in the presence of iMiD treatment. Using the ELISA procedure described previously, measurement of TNF-α levels in CRBN KO clones versus non-targeting sgRNA (NTG) clones led to a variable mixture of results (Figure 6b). The two control NTG clones exhibited differential sensitivities to iMiD treatment, with a significantly larger inhibition of TNF-α secretion observed in NTG clone 1 compared to NTG clone 4. Moreover, the four CRBN KO clones displayed an inconsistent pattern of TNF-α effects in the presence of iMiD treatment. TNF-α levels did not change with drug treatment in CRBN KO clone 2.7, while CRBN KO clones 2.5, 2.10, and 2.12 appeared to have varying degrees of partial iMiD responsiveness (Figure 6b). In aggregate, these results suggest that iMiD-induced TNF-α downregulation may plausibly occur via a CRBN-dependent mechanism. However, due to clonal heterogeneity and poor intra-assay precision, additional refinement of our model system is warranted before further studies are performed to characterize the inhibitory TNF-α effect exerted by iMiDs.

6 DISCUSSION

The recent discovery that iMiDs act by modulating the substrate specificity of an E3 ubiquitin ligase complex has been regarded as a pioneering advance for describing the first novel drug mechanism in several decades. Until this discovery, drug-mediated targeting of zinc-finger transcription factors such as IKZF1 and IKZF3 was deemed impossible because these proteins exhibited “undruggable” characteristics [87]. Achieving a comprehensive understanding of the molecular mechanisms underlying iMiD activity provides the opportunity to generate newer analogs of these drugs that are safer, more potent, and capable of targeting previously undruggable proteins. Furthermore, continued exploration of this unique pharmacological mechanism could ultimately lead to the development of novel drugs that enhance iMiD activity via complementary modulation of other ubiquitination and proteasomal degradation pathways.

6.1 FUNCTIONAL DISSECTION OF CRBN-CRL4 SUBSTRATE DEGRONS

The first part of the present study aimed to investigate iMiD mechanisms of action by characterizing the degron sequences in CRBN-CRL4 substrates that are essential for mediating drug responsiveness. Previous work from our lab has shown that zinc finger domain 2 of IKZF3 contains a sequence of amino acids that is both necessary and sufficient for conferring sensitivity to iMiD-targeted substrate degradation [63]. Through site-specific mutagenesis and a fluorescent reporter assay, our work led to the identification of single residues within the IKZF3 degron sequence that are critical for mediating recognition by the iMiD-CRBN complex. Single amino acid substitutions at Q147, C148, G152, A153, and H164 caused statistically significant impairment of degradation, as measured by fluorescent reporter expression, in the presence of iMiD treatment (Figure 2c). In addition to IKZF3, we characterized a homologous region in zinc finger domain 4 of ZFP91 and identified critical residues in this putative degron sequence using

a similar approach. Here, degradation of ZFP91 by iMiDs was blocked by single amino acid substitutions at Q401 and G406 (Figure 4c). These findings demonstrate that both established and novel CRBN-CRL4 substrates share common structural motifs characterized at the level of single amino acid residues that play a crucial role in mediating iMiD activity. Attaining a precise understanding of iMiD-sensitive degrons may help identify novel CRBN-CRL4 substrates via degron sequence homology, thereby contributing to the discovery of new molecular targets that could shed light on the currently unexplained aspects of iMiD biology.

The fluorescent reporter assay used for degron characterization in this study proved to be a highly robust and sensitive tool for interrogating the effects of degron point mutations on iMiD-induced substrate degradation. The results from this assay facilitated statistically significant conclusions regarding the functional effects of single amino acid substitutions at critical residues identified in the degron sequences of CRBN-CRL4 substrates. However, the information provided by these findings was limited to the primary level of protein structure. Additional information about protein structure at the secondary, tertiary, and quaternary levels is necessary in order to achieve a complete understanding of the factors that influence substrate recognition by the iMiD-CRBN complex. The conformational effects of single amino acid substitutions on interactions between iMiDs, CRBN, and target substrates is best obtained by the resolution of a three-dimensional crystal structure, as done previously for the iMiD-CRBN complex bound to DDB1 and CK1 α [72-74]. While the nature of interactions between established substrates (e.g. IKZF1, IKZF3) and the iMiD-CRBN complex is reasonably well-understood, further investigation is warranted to determine how specific degron residues and motifs of novel targets including ZFP91 mediate substrate recognition in the context of higher-level protein structure.

In the future, the work presented here regarding the characterization of iMiD-sensitive degrons could be extended in several directions. First, it would be highly informative to study the degron sequences present in additional CRBN-CRL4 substrates, with a particular emphasis

on novel zinc-finger protein targets such as RNF166 and ZNF692. Based on the approach used for ZFP91, homologous degron regions in these proteins could be identified and analyzed by a fluorescent reporter assay in order to determine the effects of site-specific mutagenesis on iMiD-induced substrate degradation. The results of this future work would reveal whether degradation of RNF166, ZNF692, and other novel substrates in the presence of iMiD treatment is dependent on the existing pattern of critical amino residues identified in the IKZF3 and ZFP91 degrons. In addition to characterizing the degron sequences present within additional substrates, another direction for related work would entail studying the degron motifs responsible for mediating sensitivity to novel iMiD analogs currently in development. For instance, CC-122 is a next-generation iMiD analog that has shown antitumor activity in diffuse large B-cell lymphoma [88]. Despite binding to the CRBN-CRL4 complex as a common target, it is possible that novel iMiD derivatives including CC-122 recruit substrates for degradation via degron sequences that have not been characterized for existing compounds. The dissection of novel degrons to identify critical amino acid residues may help reveal the structural basis for differential targeting of CRBN-CRL4 substrates by individual iMiD derivatives.

Recent crystallography of the iMiD-CRBN complex has provided structural insight into aspects of iMiD biology that have previously eluded a mechanistic rationale. For example, the crystallization of the CRBN-DDB1-lenalidomide-CK1 α complex demonstrated that the selective activity of lenalidomide versus other iMiD derivatives in del(5q)-MDS arises from a favorable steric interaction facilitated by the absence of a C3 carbonyl group on the drug's phthalimide ring [74]. Moreover, crystallization of the CRBN–DDB1–CC-885–GSPT1 complex has shown that GSPT1 binds to CRBN via a structural motif similar to IKZF1, further endorsing the paradigm of degron-mediated substrate recruitment to the CRBN-CRL4 E3 ligase [89]. In contrast to the established CRBN-CRL4 substrates, our understanding of the structural determinants underlying the interaction between iMiDs and newly identified zinc-finger protein targets

including ZFP91, ZNF692, and RNF166 remains limited. In this study, we found that degradation of ZFP91 is most strongly induced by pomalidomide in comparison to lenalidomide or thalidomide. However, the absence of a crystal structure for the iMiD-CRBN complex bound to ZFP91 limits our molecular understanding of this observation. Future efforts directed toward solving a crystal structure for the CRBN-pomalidomide-ZFP91 complex could provide a structural basis for the differential substrate specificities exerted by iMiD family members in targeting this substrate. More broadly, crystallographic analysis would further elucidate the conformational dynamics of complex formation between iMiDs, CRBN, and other novel zinc-finger protein substrates.

6.2 Investigation of the Molecular Basis for iMiD-Induced TNF-α Downregulation

The second part of the present study sought to describe a molecular mechanism for the iMiD-induced effect of TNF-α downregulation in monocytes. Although thalidomide was first shown to inhibit TNF-α in 1991, a precise molecular understanding of this effect has evaded researchers for more than two decades [78]. Clinically, TNF-α inhibition is thought to be responsible for the therapeutic efficacy of iMiDs in the treatment of erythema nodosum leprosum. Moreover, lenalidomide and pomalidomide were optimized as newer analogs of thalidomide to exhibit enhanced immunomodulatory properties, one of which included increased potency of TNF-α inhibition [37]. Given that TNF-α inhibition remains a poorly understood facet of iMiD biology, elucidation of the molecular mechanism underlying this effect could potentially lead to the development of novel iMiD derivatives optimized to treat TNF-mediated inflammatory diseases including rheumatoid arthritis, inflammatory bowel disease, and psoriasis [90].

We examined the TNF-α effect of iMiDs by generating CRISPR/Cas9-mediated single-cell knockout clones in the pro-monocytic U937 cell line in order to targeted known components of

the CRBN-CRL4 degradation pathway. Our strategy involved generating knockout clones with sgRNAs targeting CRBN, established CRBN-CRL4 substrates (IKZF1, IKZF3, and CK1α), and novel CRBN-CRL4 substrates (ZFP91, ZNF692, and RNF166). All clones were analyzed by deep sequencing in order to confirm the presence of inactivating out-of-frame indels induced by CRISPR/Cas9. Following knockout validation, clones were phenotypically characterized using an ELISA-based approach. Specifically, clones were subjected to PMA-induced macrophagic differentiation, treated with iMiDs, and stimulated with LPS to enhance TNF-α secretion. Supernatants were analyzed by ELISA to determine whether genetic inactivation of a particular target affected TNF-α levels in the presence and absence of iMiD treatment.

Given that one CRBN KO clone demonstrated complete abrogation of iMiD-induced TNF-α inhibition and the remaining CRBN KO clones demonstrated partial iMiD responsiveness, our results suggest a plausible CRBN-dependent mechanism for this biological effect. However, our results are not fully conclusive due to a number of limitations encountered with experimental system used in this study. First, interpretation of the TNF-α assay was limited by poor precision, as evident by large error bars with significant variability among technical replicates. Moreover, another limitation of the assay was variability among biological replicates due to clonal heterogeneity. TNF-α levels in the control NTG clones exhibited variable responsiveness to iMiD treatment, rendering it difficult to interpret results of the assay in the absence of a reliable baseline. CRBN KO clones also responded inconsistently to iMiD treatment, as seen with the absence of iMiD sensitivity in one CRBN KO clone and varying degrees of partial iMiD sensitivity observed in three CRBN KO clones. This pattern of results could suggest that the heterogeneity between single-cell clones outweighs the biological effects of iMiDs detectable in our experimental system. Finally, although less likely, these results potentially raise the question of a CRBN-independent mechanism for iMiD-induced TNF-α downregulation. Despite countering our original hypothesis that the TNF-α effect is dependent on the CRBN pathway and its known

substrates, this theory would align with a recent report by Millrine *et. al*. claiming that iMiDs inhibit secretion of TLR-inducible cytokines including TNF-α independently of CRBN through suppression of the TRIF/IRF3 pathway [91]

Future efforts should be focused on selecting and refining an appropriate model system to study the mechanistic basis for TNF-α inhibition by iMiDs. One way to improve our current model would be to consider the use of additional human pro-monocytic cell lines such as THP-1, HL-60, and Kasumi-1. Although the parental U937 cell line was moderately sensitive to iMiD treatment, it is possible that another cell line would also be iMiD-responsive without exhibiting the same degree of clonal heterogeneity following the single-cell cloning process. In addition to considering alternate cell lines, this system could be refined by making efforts to minimize assay variability arising from technical sources. Some potential approaches could involve increasing the number of technical replicates and normalizing ELISA measurements to total protein content in lysed samples. Quantitative PCR could be used as an alternate readout assay to measure TNF-α expression with more reliability than ELISA, given the standard inclusion of reference genes (e.g. GAPDH) as internal controls. Finally, it is plausible that selecting candidate target genes from known CRBN-CRL4 pathway members and generating CRISPR/Cas9-mediated knockout clones is too simplistic of an approach to fully dissect the complexity of TNF-α blockade by iMiDs. As an alternative approach, we would consider performing a SILAC-based quantitative mass spectrometry experiment to analyze the proteome and ubiquitome of an appropriate monocytic cell line in the presence of iMiD treatment. Previous proteomics experiments in MM.1S and KG-1 cells successfully revealed IKZF1/IKZF3 and CK1α as the molecular targets of iMiD activity in multiple myeloma and del(5q)-MDS, respectively [63,66]. Similarly, by detecting global changes in protein abundance and ubiquitination, this experiment would offer a broad, unbiased approach to identify novel targets specific to the monocytic niche yet to be considered as mechanistic drivers of iMiD-induced TNF-α inhibition.

7 CONCLUSIONS

In the present study, characterization of CRBN-CRL4 substrate degrons led to the identification of amino acid residues that play a critical role in mediating iMiD sensitivity. Single amino acid substitutions at residues Q147, C148, G152, A153, and H164 located in zinc finger domain 2 of IKZF3 abrogated substrate degradation in a flow cytometry-based fluorescent reporter assay. Similarly, single amino acid substitutions at residues Q401 and G406 located in zinc finger domain 4 of ZFP91 also blocked iMiD-induced degradation. These results indicate that CRBN-CRL4 substrates targeted by iMiDs contain shared amino acid motifs that function as necessary and sufficient signals for drug-induced degradation. Future work in this area should examine the structural biology of iMiD-inducible degron motifs. Specifically, solving of a CRBN-iMiD-ZFP91 crystal structure would help elucidate the structural determinants underlying recognition of novel zinc-finger protein substrates by the iMiD-CRBN complex.

Our efforts to study iMiD-induced TNF-α inhibition via generation of CRISPR/Cas9 single-cell knockout clones suggested a plausible CRBN-dependent mechanism. However, conclusive interpretation of results obtained from testing of CRBN knockout clones was limited by poor intra-assay precision and clonal heterogeneity. Future efforts to study this question should address the limitations of our current model system. Potential improvements include using another cell line, minimizing biological and technical variability, and selecting an alternative readout assay. Finally, the overall experimental approach could be modified to consider an unbiased method of target identification. For instance, a SILAC-based proteomics experiment performed in drug-treated monocytes could reveal novel substrates specific to this cell type that uncover the presently elusive molecular basis for TNF-α inhibition by iMiDs.

8 SUMMARY

The overarching goal of the work presented here was to elucidate the molecular mechanisms for inadequately characterized aspects of iMiD biology. Our first aim was to describe how the iMiD-CRBN complex targets substrates for degradation via conserved amino acid motifs known as degrons. Our second aim was to investigate the mechanism for iMiD-induced TNF-α downregulation, a key biological effect of this class of pharmacological agents that has eluded a molecular explanation for more than two decades.

Degron studies were performed by analyzing the effects of single amino acid substitutions on iMiD-induced CRBN-CRL4 substrate degradation via a flow cytometry-based fluorescent reporter assay. Site-specific mutagenesis of degrons located in zinc-finger domain 2 of IKZF3 and zinc-finger domain 4 of ZFP91 identified the presence of critical amino acid residues that are necessary for conferring iMiD responsiveness. Although these results provided functional insight into the amino acid motifs within iMiD-inducible degrons, structural biology approaches (e.g. X-ray crystallography) are needed to achieve a complete understanding of the conformational interactions between iMiDs, target substrates, and the CRBN-CRL4 E3 ubiquitin ligase complex.

Mechanistic investigation of iMiD-induced TNF-α downregulation was conducted by generating CRISPR/Cas9-mediated single-cell knockout clones to inactivate known factors associated with the CRBN-CRL4 complex. The results of preliminary experiments suggest a plausible CRBN-dependent mechanism for this effect. Further efforts to refine our model system are necessary to address clonal heterogeneity and assay variability before proceeding with additional studies. In the future, an unbiased proteomics approach should be considered as an alternative method to interrogate the molecular mechanism of iMiD-associated TNF-α blockade.

9 ACKNOWLEDGMENTS

I would like to thank Dr. Benjamin Ebert for his always kind support and mentorship during my research year and beyond. I would like to thank Quinlan Sievers for his guidance and collaboration in addition to all members of the Ebert Lab who provided assistance in the completion of this project. This work was funded by a Physician-Scientist Career Development Award from the American Society of Hematology (S.D.H).

Lastly, I would like to dedicate this thesis to both of my parents, Subrata and Aruna Haldar, whose tireless devotion to the scientific profession has always served as an inspiration for my pursuit of an investigative career in academic medicine.

10 TABLES

System/Process	Effect	Associated Disorders	Molecular Target(s)
Carcinogenesis	Destruction of the malignant clone	Multiple myeloma del(5q)-MDS Mantle cell lymphoma Solid tumors (e.g. GBM, RCC, Kaposi's sarcoma)	Ikaros (IKZF1), Aiolos (IKZF3) Casein kinase 1A1 (CK1α) Others may be unknown.
Immune System	Decreased TNF-α secretion Increased IL-2 secretion	Erythema nodosum leprosum HIV-associated aphthous ulcers Crohn's disease Systemic lupus erythematosus Graft-versus-host disease	Unknown
Central Nervous System	Sedative	Side effect	Unknown
Peripheral Nervous System	Peripheral neuropathy	Side effect	Unknown
Embryogenesis	Teratogenicity	Side effect	Unknown
Hemostasis	Increased risk of venous thromboembolism	Side effect	Unknown
Vascular System	Inhibition of angiogenesis	Cancer?	Unknown

Table 1. ***Pleiotropic Biological Activities of iMiDs*** [adapted from Quinlan Sievers]

Target Gene	sgRNA sequences
CSNK1A1	1) GATCAACATCACCAACGGCGAGG 2) AGGCTGAATTCATTGTCGGAGGG
CRBN	1) GCACCATACTGACTTCTTGAGGG 2) ATGGTGGCAGAAATACCAGAAGG
IKZF1	1) TGAGCCCATGCCGATCCCCGAGG 2) CTTCCAGTGCAATCAGTGCGGGG
IKZF3	1) GATAGTAGCAGGCCAACCAGTGG 2) CCACATTAAACTGCACACAGGGG
RNF166	1) TGTGCCCTGCAGGTTCTGCGGGG 2) CCCTTCGACCCCAAGAAGGTGGA
ZFP91	1) GCTGCATCTAGACCTAGCCGGGG 2) TCAGGGAAACCCCAAAGCCACGG
ZNF692	1) GCAGGCGGCGGGAGAAGCGGCGG 2) GCATGATGAGAGGACTCAAGAGG

Table 2. ***sgRNA Sequences for CRISPR/Cas9-Mediated Target Gene Knockout***

sgRNA Name	Forward Primer (5' to 3')	Reverse Primer (5' to 3')
CSNK1A1 sgRNA #1	GGCTCCTTCGGGGACATCTA	ACGAGGTTCGTAAGCCAGGAA
CSNK1A1 sgRNA #2	GGCTCCTTCGGGGACATCTA	ACGAGGTTCGTAAGCCAGGAA
CRBN sgRNA #1	CATGGCAGGACTTTGCACG	CCCATGAGAGGGAATGTATTAAGC
CRBN sgRNA #2	TGCAGTTCAATTAGAATCCCTCA	AACTCAAGAGCCGAACATCTAA
IKZF1 sgRNA #1	TCCTCATGCCACCCTCTCAA	TGCCAGTTGAGGGAACACAA
IKZF1 sgRNA #2	CTCATGTTCTATCAAACCTGCAGCC	AGGGGACCTACCGGAGTGC
IKZF3 sgRNA #1	AGAATGTTTTAAAGTCAGAACCCAT	CCAAAAGTTCCAAATTCCACCACT
IKZF3 sgRNA #2	GAGCTTTTCCCCTAGGCATCT	CACACTGGGCTCTGAGGAAT
RNF166 sgRNA #1	CCACAAATGCTGGGTCCTAAG	GGCTGCCCATCAAGTGACC
RNF166 sgRNA #2	TGCCTGCAGGTGCCATC	CCGTCACCACAGGAAGTGAG
ZFP91 sgRNA #1	CAAGGAAGAAAAAGAGGAAGAAGAC	CCTGACAGTTAAGCTGTTAACACAA
ZFP91 sgRNA #2	TGTTGTCATAGTCTTCCTTGAAAAG	ACCTTCTCCTTGCAATAGAACTGA
ZNF692 sgRNA #1	TCTGGTGCACATGGCTTCCTC	GCCCTGGGCACTCACAC
ZNF692 sgRNA #2	TTCCTTCTCTTTTGACTTTGCCT	TCTTTTTGCCTTCCCCAAAACC

Table 3. ***Primer Sequences for Detection of CRISPR/Cas9-Induced Indels in Target Genes***

11 FIGURES

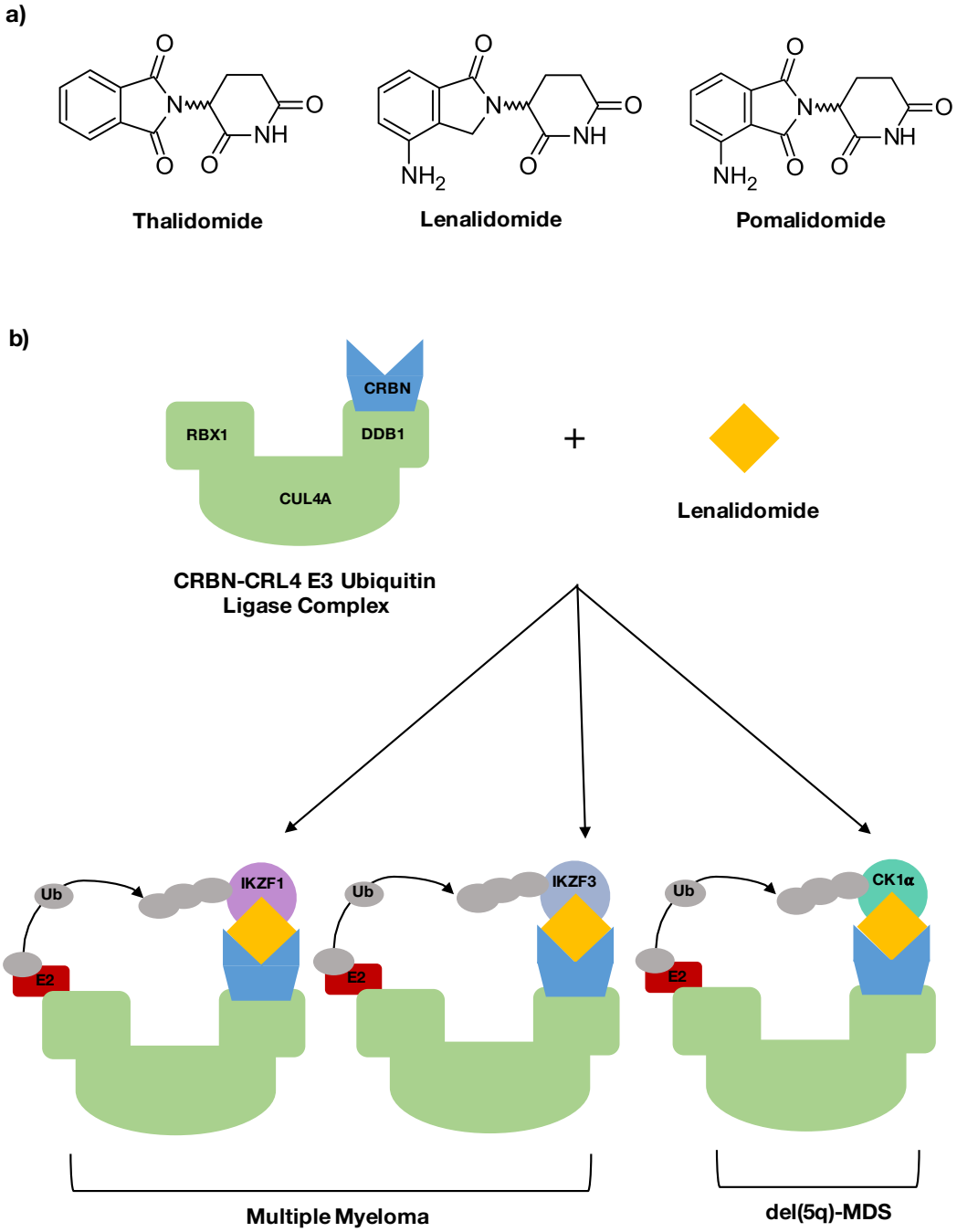

Figure 1. ***Structural and Mechanistic Properties of iMiDs.*** a) Chemical structures of iMiDs. Each compound consists of a glutarimide ring linked to a phthalimide moiety with differing amino and carbonyl group substitutions. b) Schematic drawing of iMiD mechanism of action [adapted from Quinlan Sievers]. Components of the CRBN-CRL4 E3 ubiquitin ligase complex include CRBN (substrate receptor), DDB1 (adaptor), CUL4A (scaffold), and RBX1 (recruits E2 ubiquitin-conjugating enzyme). iMiDs bind to the substrate adaptor CRBN and alter the specificity of this complex to target individual substrates for ubiquitin-mediated proteasomal degradation. Targeted substrates include IKZF1/IKZF3 in MM and CK1 α in del(5q)-MDS.

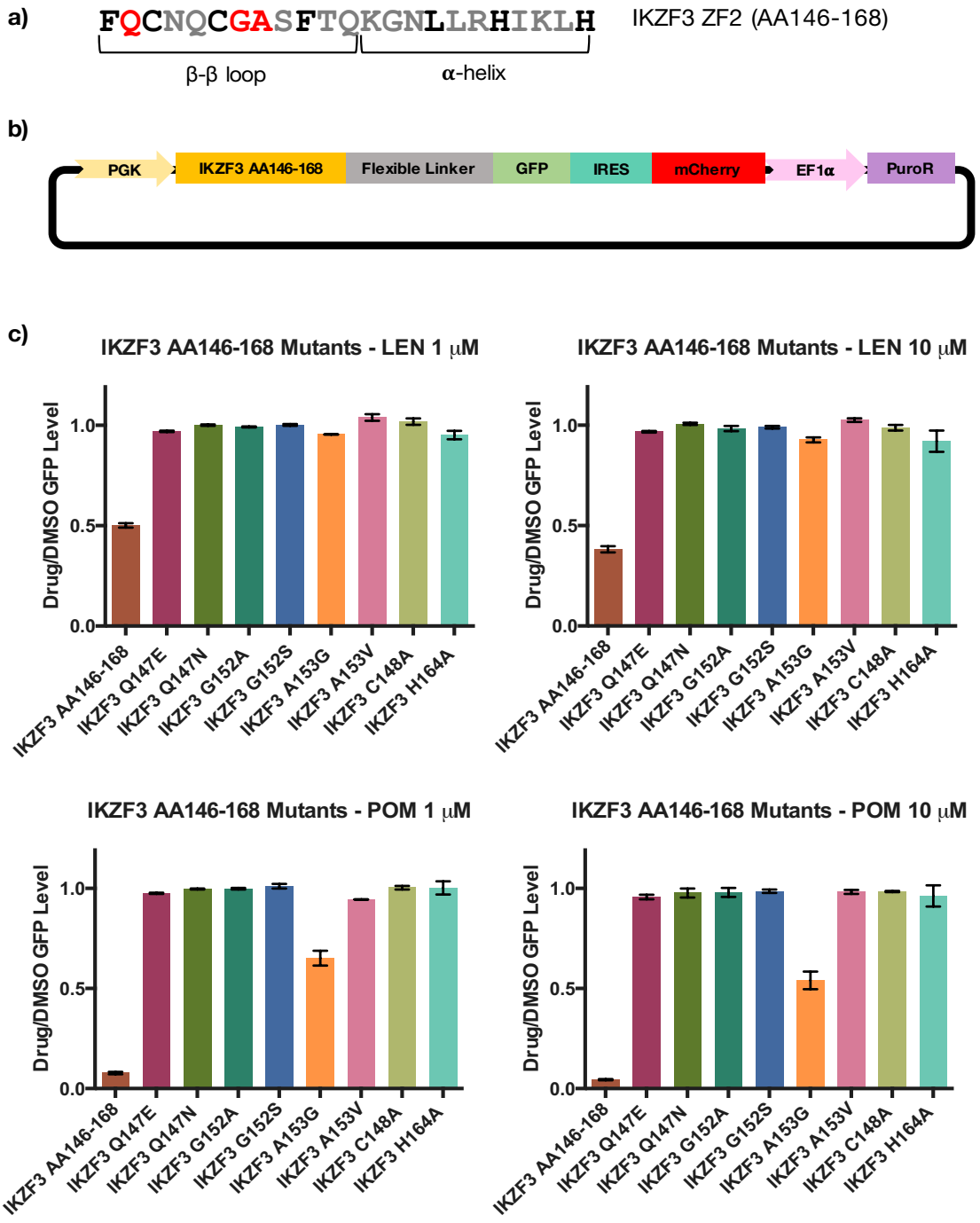

Figure 2. ***Effects of IKZF3 Degron Mutagenesis on Substrate Recognition by the iMiD-CRBN Complex.*** a) Amino acid sequence of the IKZF3 C2H2 zinc finger 2 domain. Black and red residues have been previously identified as necessary for mediating iMiD-induced degradation, with black denoting residues conserved in C2H2 zinc finger motif and red denoting non-conserved residues unique to the IKZF3 degron. b) Schematic diagram of fluorescent reporter vector containing IKZF3 AA146-168 fused to GFP via a flexible linker. c) Analysis of IKZF3 AA146-168 point mutants via a flow cytometry-based fluorescent reporter assay. HEK293T cells were transfected with reporter vectors expressing wild-type and mutant IKZF3 degron sequences and treated for 18 h with 0.1% DMSO and the indicated doses of lenalidomide and pomalidomide. Flow cytometry was used to measure GFP expression following drug treatment. Drug/DMSO GFP levels are reported as an average of three technical replicates +/- s.e.m.

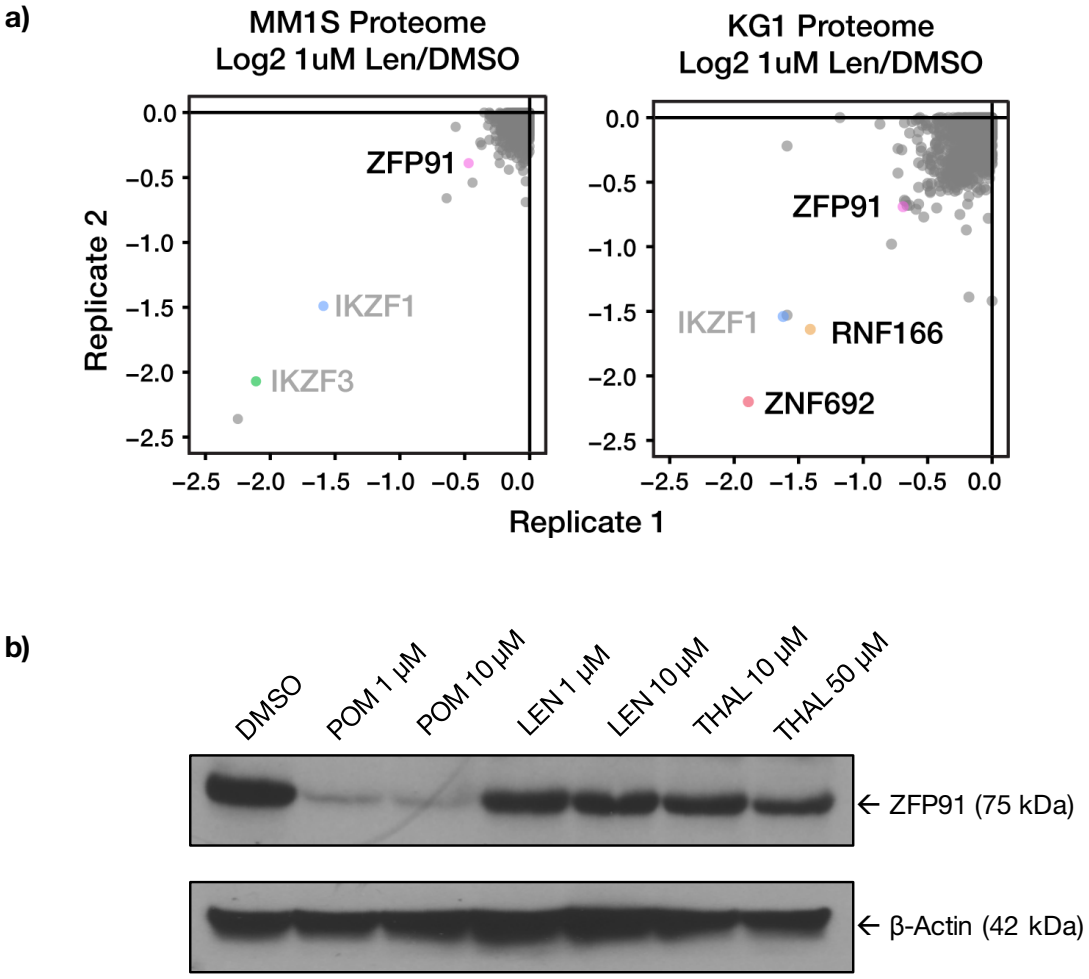

Figure 3. ***Validation of ZFP91 as a Novel CRBN-CRL4 E3 Ubiquitin Ligase Substrate.*** a) SILAC-based proteome-wide profiling of MM.1S and KG-1 cells following lenalidomide treatment for 12 h [63,66]. Novel CRBN-CRL4 substrates ZFP91, ZNF692, and RNF166 are highlighted with bold text. b) KG-1 cells were treated for 18 h with 0.1% DMSO and the indicated doses of thalidomide, lenalidomide, and pomalidomide. Protein lysates were analyzed via Western immunoblotting for detection of endogenous ZFP91 levels in the presence of drug treatment. Detection of β-actin served as the loading control.

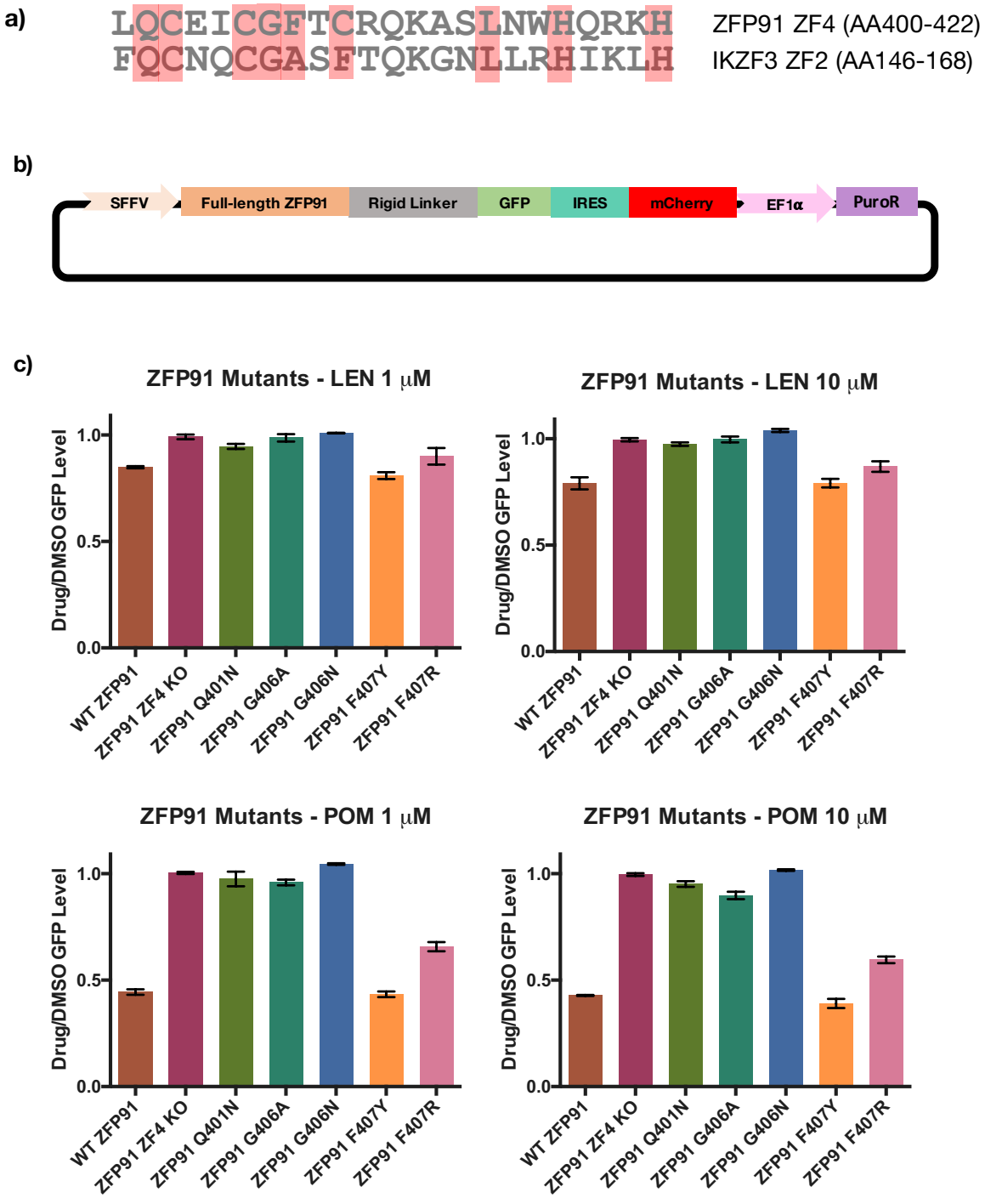

Figure 4. ***Effects of ZFP91 Degron Mutagenesis on Substrate Recognition by the iMiD-CRBN Complex***. a) Amino acid sequence of ZFP91 zinc finger domain 4 (ZF4) aligned to the IKZF3 C2H2 zinc finger domain 2 (ZF2). b) Schematic diagram of fluorescent reporter vector containing full-length ZFP91 fused to GFP via a rigid linker. c) Analysis of ZFP91 ZF4 point mutants via a flow cytometry-based fluorescent reporter assay. HEK293T cells were transfected with reporter vectors expressing wild-type and mutant ZFP91 degron sequences and treated for 18 h with 0.1% DMSO and the indicated doses of lenalidomide and pomalidomide. Flow cytometry was used to measure GFP expression following drug treatment. Drug/DMSO GFP levels are reported as an average of three technical replicates +/- s.e.m.

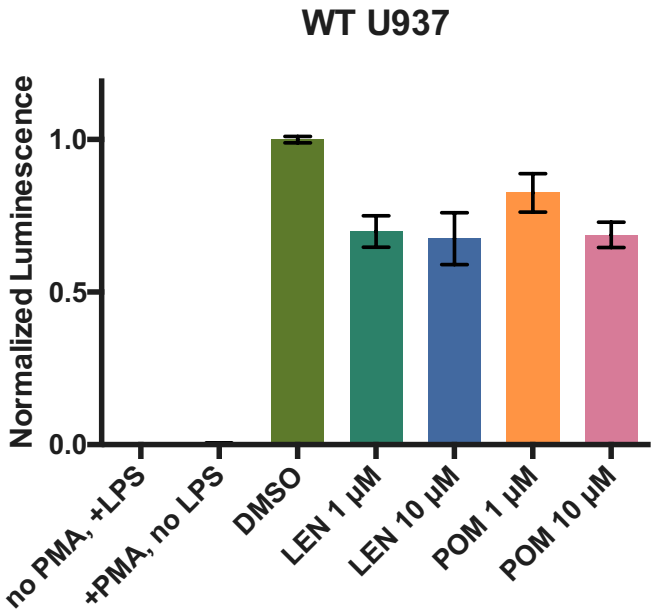

Figure 5. ***iMiD-Induced TNF-α Downregulation in U937 Monocytic Cells.*** U937 cells were seeded at a density of 5 x 10^4 cells per well in a 96-well plate and treated with PMA for 24 h to induce differentiation into a macrophage-like state. Following PMA-induced differentiation, cells were treated for 18 h with 0.1% DMSO, lenalidomide, or pomalidomide at the indicated doses. 4 h after drug treatment, cells were stimulated with 100 ng/mL LPS for a duration of 16 h. Cells not treated with LPS or PMA served as negative controls. TNF-α levels were quantified in harvested supernatants by chemiluminescent ELISA with results reported as a normalized average of three technical replicates +/- s.e.m.

a)

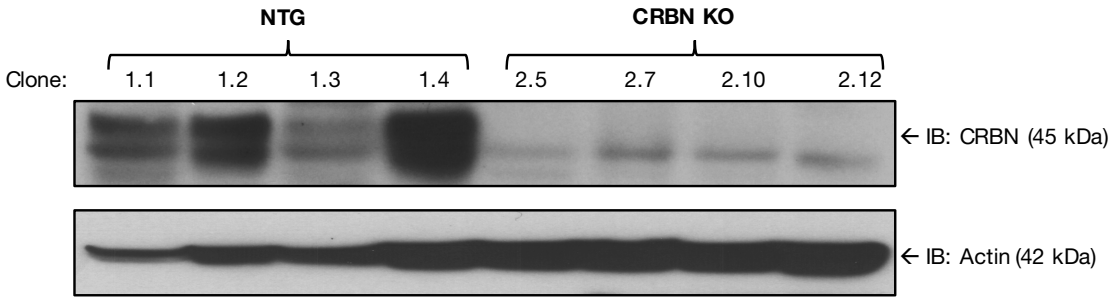
NTG
CRBN KO
Clone:
1.1
1.2
1.3
1.4
2.5
2.7
2.10
2.12
← IB: CRBN (45 kDa)
← IB: Actin (42 kDa)

b)

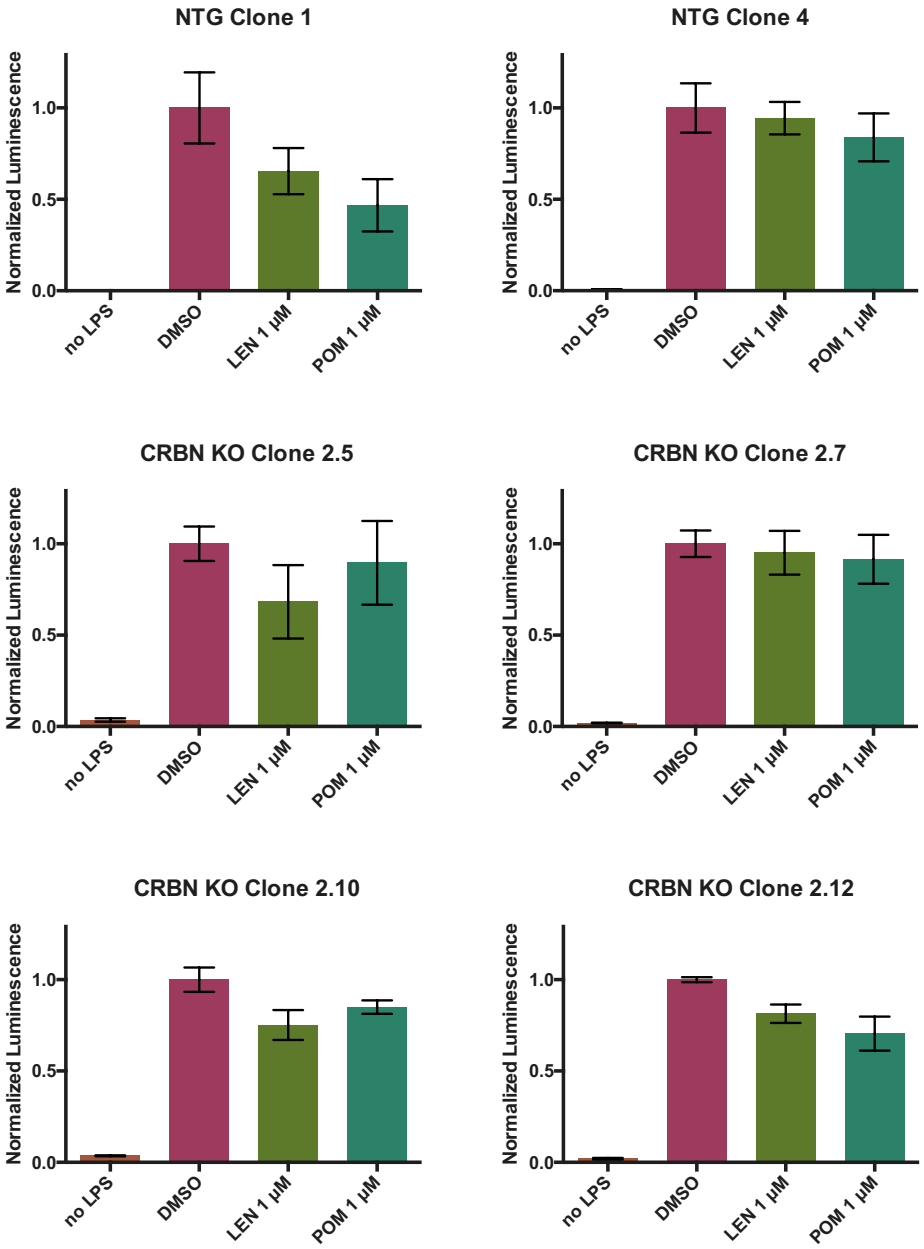
NTG Clone 1
NTG Clone 4
CRBN KO Clone 2.5
CRBN KO Clone 2.7
CRBN KO Clone 2.10
CRBN KO Clone 2.12
Normalized Luminescence
0.0
0.5
1.0
no LPS
DMSO
LEN 1 µM
POM 1 µM

Figure 6. ***Effects of CRISPR/Cas9-Mediated CRBN Inactivation on iMiD-Induced TNF-α Downregulation.*** a) Validation of U937 single-cell CRBN knockout clones via Western immunoblotting. Protein lysates were prepared from clones shown by deep sequencing to have CRISPR/Cas9-mediated out-of-frame indels in CRBN Exon 5. Expression of CRBN was detected using standard Western immunoblotting procedures and compared to control lysates prepared from non-targeting sgRNA (NTG) clones. b) Analysis of TNF-α levels in single-cell CRBN knockout clones by chemiluminescent ELISA. CRBN KO and NTG clones were seeded in a 96-well plate and treated with PMA for 24 h to induce macrophagic differentiation. Treatment with 0.1% DMSO, 1 μM lenalidomide, or 1 μM pomalidomide was performed after the completion of PMA-induced differentiation. 4 h post-drug treatment, clones were stimulated for 16 h with 100 ng/mL LPS. Cells not treated with LPS served as the negative control. Supernatants were harvested for measurement of TNF-α levels via chemiluminescent ELISA. Results are reported as a normalized average of three technical replicates +/- s.e.m.

REFERENCES

1. Richardson P, Hideshima T, Anderson K. Thalidomide: emerging role in cancer medicine. Annu Rev Med. 2002;53(1):629–657. PMID: 11818493

2. Calabrese L, Fleischer AB. Thalidomide: current and potential clinical applications. Am J Med. 2000 Apr 15;108(6):487–495. PMID: 10781782

3. Bartlett JB, Dredge K, Dalgleish AG. The evolution of thalidomide and its IMiD derivatives as anticancer agents. Nat Rev Cancer. Nature Publishing Group; 2004 Apr;4(4):314–322. PMID: 15057291

4. McBride W. Thalidomide and congential malformation. Lancet. Lancet; 1961.

5. Lenz W, Pfeiffer RA, Kosenow W, Hayman DJ. Thalidomide and congenital abnormalities. Lancet. The Lancet; 1962.

6. Singhal S, Mehta J, Desikan R, Ayers D, Roberson P, Eddlemon P, Munshi N, Anaissie E, Wilson C, Dhodapkar M, Zeldis J, Siegel D, Crowley J, Barlogie B. Antitumor activity of thalidomide in refractory multiple myeloma. N Engl J Med. Massachusetts Medical Society; 2008 Oct 21;341(21):1565–1571. PMID: 10564685

7. List A, Dewald G, Bennett J, Giagounidis A, Raza A, Feldman E, Powell B, Greenberg P, Thomas D, Stone R, Reeder C, Wride K, Patin J, Schmidt M, Zeldis J, Knight R. Lenalidomide in the myelodysplastic syndrome with chromosome 5q deletion. N Engl J Med. Massachusetts Medical Society; 2009 Oct 8;355(14):1456–1465.

8. Keller H, Kunz W, Muckter H. N-phthalyl-glutamic acid imide; experimental studies on a new synthetic product with sedative properties. Arzneimittel-Forschung; 1956 Aug 1;6(8):426–430. PMID: 13373636

9. Stephens T, Brynner R. Dark Remedy: The Impact of Thalidomide and Its Revival as a Vital Medicine Basic Books; 2009.

10. Somers GF. Pharmacological properties of thalidomide (alpha-phthalimido glutarimide), a new sedative hypnotic drug. British Journal of Pharmacology and Chemotherapy. Blackwell Publishing Ltd; 1960 Mar 1;15(1):111–116.

11. Rajkumar SV. Thalidomide: tragic past and promising future. Mayo Clinic Proceedings. Elsevier; 2004 Jul 1;79(7):899–903.

12. Mann RD. Modern Drug Use. Dordrecht: Springer Science & Business Media; 2012.

13. Florence AL. Is thalidomide to blame? British Medical Journal. BMJ Group; 1960 Dec 31;2(5217):1954. PMCID: PMC2098660

14. Mellin GW, Katzenstein M. The saga of thalidomide: neuropathy to embryopathy, with case reports of congenital anomalies. N Engl J Med. 1962.

15. Smithells RW, Newman CG. Recognition of thalidomide defects. Journal of Medical Genetics. BMJ Group; 1992 Oct;29(10):716–723. PMCID: PMC1016130

16. Lenz W. A short history of thalidomide embryopathy. Birth Defects Research Part A: Clinical and Molecular Teratology. Wiley Subscription Services, Inc., A Wiley Company; 1988 Sep 1;38(3):203–215.

17. Watts G. Frances Oldham Kelsey. Lancet. Elsevier; 2015 Oct 3;386(10001):1334. PMID: 26460767

18. Wemambu SN, Turk JL, Waters MF, Rees RJ. Erythema nodosum leprosum: a clinical manifestation of the arthus phenomenon. Lancet. 1969 Nov 1;2(7627):933–935. PMID: 4186599

19. Sheskin J. THALIDOMIDE IN THE TREATMENT OF LEPRA REACTIONS. Clinical Pharmacology and Therapeutics. 1965 May;6:303–306. PMID: 14296027

20. Sampaio EP, Kaplan G, Miranda A, Nery JA, Miguel CP, Viana SM, Sarno EN. The influence of thalidomide on the clinical and immunologic manifestation of erythema nodosum leprosum. J Infect Dis. 1993 Aug;168(2):408–414. PMID: 8335978

21. Iyer CG, Languillon J, Ramanujam K, Tarabini-Castellani G, las Aguas De JT, Bechelli LM, Uemura K, Martinez Dominguez V, Sundaresan T. WHO co-ordinated short-term double-blind trial with thalidomide in the treatment of acute lepra reactions in male lepromatous patients. Bull World Health Organ. World Health Organization; 1971;45(6):719–732. PMCID: PMC2427977

22. U.S. Food and Drug Administration. NDA 20-785 [Internet]. accessdata.fda.gov. 1998 [cited 2016 Jun 2]. Available from: http://www.accessdata.fda.gov/drugsatfda_docs/appletter/1998/20785ltr.pdf

23. Bach MC, Valenti AJ, Howell DA, Smith TJ. Odynophagia from aphthous ulcers of the pharynx and esophagus in the acquired immunodeficiency syndrome (AIDS). Ann Intern Med. 1988 Aug 15;109(4):338–339. PMID: 3395042

24. Lähdevirta J, Maury CP, Teppo AM, Repo H. Elevated levels of circulating cachectin/tumor necrosis factor in patients with acquired immunodeficiency syndrome. Am J Med. 1988 Sep;85(3):289–291. PMID: 3414726

25. Poli G, Kinter A, Justement JS, Kehrl JH, Bressler P, Stanley S, Fauci AS. Tumor necrosis factor alpha functions in an autocrine manner in the induction of human immunodeficiency virus expression. Proc Natl Acad Sci USA. 1990 Jan;87(2):782–785. PMCID: PMC53350

26. Jacobson JM, Greenspan JS, Spritzler J, Ketter N, Fahey JL, Jackson JB, Fox L, Chernoff M, Wu AW, MacPhail LA, Vasquez GJ, Wohl DA. Thalidomide for the treatment of oral aphthous ulcers in patients with human immunodeficiency virus infection. National Institute of Allergy and Infectious Diseases AIDS Clinical Trials Group. N Engl J Med. 1997 May 22;336(21):1487–1493. PMID: 9154767

27. Thompson C. Thalidomide effective for AIDS-related oral ulcers. Lancet. 1995 Nov 11;346(8985):1289. PMID: 7475726

28. D'Amato RJ, Loughnan MS, Flynn E, Folkman J. Thalidomide is an inhibitor of angiogenesis. Proc Natl Acad Sci USA. National Academy of Sciences; 1994 Apr 26;91(9):4082–4085. PMCID: PMC43727

29. Stolberg SG. Thalidomide Found to Slow a Bone Cancer. NY Times. 1999 Nov 18.

30. Chanan-Khan AAA. Immunomodulating Drugs for the Treatment of Cancer. Lippincott Williams & Wilkins; 2012.

31. Rajkumar SV, Blood E, Vesole D, Fonseca R, Greipp PR, Eastern Cooperative Oncology Group. Phase III clinical trial of thalidomide plus dexamethasone compared with dexamethasone alone in newly diagnosed multiple myeloma: a clinical trial coordinated by the Eastern Cooperative Oncology Group. J Clin Oncol. American Society of Clinical Oncology; 2006 Jan 20;24(3):431–436. PMID: 16365178

32. Wijermans P, Schaafsma M, Termorshuizen F, Ammerlaan R, Wittebol S, Sinnige H, Zweegman S, van Marwijk Kooy M, van der Griend R, Lokhorst H, Sonneveld P, Dutch-Belgium Cooperative Group HOVON. Phase III study of the value of thalidomide added to melphalan plus prednisone in elderly patients with newly diagnosed multiple myeloma: the HOVON 49 Study. J Clin Oncol. American Society of Clinical Oncology; 2010 Jul 1;28(19):3160–3166. PMID: 20516439

33. Cavo M, Pantani L, Pezzi A, Petrucci MT, Patriarca F, Di Raimondo F, Marzocchi G, Galli M, Montefusco V, Zamagni E, Gamberi B, Tacchetti P, Brioli A, Palumbo A, Sonneveld P. Bortezomib-thalidomide-dexamethasone (VTD) is superior to bortezomib-cyclophosphamide-dexamethasone (VCD) as induction therapy prior to autologous stem cell transplantation in multiple myeloma. Leukemia. 2015 Dec;29(12):2429–2431. PMID: 26442610

34. U.S. Food and Drug Administration. FDA approves Thalomid (thalidomide) to treat multiple myeloma [Internet]. Center for Drug Evaluation and Research; [cited 2016 Jun 2]. Available from: http://www.fda.gov/AboutFDA/CentersOffices/OfficeofMedicalProductsandTobacco/CDER/ucm095651.htm

35. Ghobrial IM, Rajkumar SV. Management of thalidomide toxicity. J Support Oncol. 2003 Sep;1(3):194–205. PMCID: PMC3134146

36. Corral LG, Haslett PA, Muller GW, Chen R, Wong LM, Ocampo CJ, Patterson RT, Stirling DI, Kaplan G. Differential cytokine modulation and T cell activation by two distinct classes of thalidomide analogues that are potent inhibitors of TNF-alpha. J Immunol. 1999 Jul 1;163(1):380–386. PMID: 10384139

37. Muller GW, Chen R, Huang S-Y, Corral LG, Wong LM, Patterson RT, Chen Y, Kaplan G, Stirling DI. Amino-substituted thalidomide analogs: Potent inhibitors of TNF-α production. Bioorganic & Medicinal Chemistry Letters. 1999 Jun;9(11):1625–1630.

38. Hideshima T, Chauhan D, Shima Y, Raje N, Davies FE, Tai YT, Treon SP, Lin B, Schlossman RL, Richardson P, Muller G, Stirling DI, Anderson KC. Thalidomide and its analogs overcome drug resistance of human multiple myeloma cells to conventional therapy. Blood. 2000 Nov 1;96(9):2943–2950. PMID: 11049970

39. Richardson PG, Schlossman RL, Weller E, Hideshima T, Mitsiades C, Davies F, LeBlanc R, Catley LP, Doss D, Kelly K, McKenney M, Mechlowicz J, Freeman A, Deocampo R, Rich R, Ryoo JJ, Chauhan D, Balinski K, Zeldis J, Anderson KC. Immunomodulatory drug CC-5013 overcomes drug resistance and is well tolerated in patients with relapsed multiple myeloma. Blood. American Society of Hematology; 2002 Nov 1;100(9):3063–3067. PMID: 12384400

40. Dimopoulos M, Spencer A, Attal M, Prince HM, Harousseau J-L, Dmoszynska A, Miguel JS, Hellmann A, Facon T, Foà R, Corso A, Masliak Z, Olesnyckyj M, Yu Z, Patin J, Zeldis JB, Knight RD. Lenalidomide plus dexamethasone for relapsed or refractory multiple myeloma. N Engl J Med. Massachusetts Medical Society; 2009 Oct 9;357(21):2123–2132. PMID: 18032762

41. Weber DM, Chen C, Niesvizky R, Wang M, Belch A, Stadtmauer EA, Siegel D, Borrello I, Rajkumar SV, Chanan-Khan AA, Lonial S, Yu Z, Patin J, Olesnyckyj M, Zeldis JB, Knight RD. Lenalidomide plus dexamethasone for relapsed multiple myeloma in north america. N Engl J Med. Massachusetts Medical Society; 2009 Oct 9;357(21):2133–2142.

42. U.S. Food and Drug Administration. FDA approves new treatment for myelodysplastic syndrome (MDS) [Internet]. [cited 2016 Jun 2]. Available from: http://www.fda.gov/NewsEvents/Newsroom/PressAnnouncements/2005/ucm108546.htm

43. Palumbo A, Hajek R, Delforge M, Kropff M, Petrucci MT, Catalano J, Gisslinger H, Wiktor-Jędrzejczak W, Zodelava M, Weisel K, Cascavilla N, Iosava G, Cavo M, Kloczko J, Bladé J, Beksac M, Spicka I, Plesner T, Radke J, Langer C, Yehuda DB, Corso A, Herbein L, Yu Z, Mei J, Jacques C, Dimopoulos MA. Continuous lenalidomide treatment for newly diagnosed multiple myeloma. N Engl J Med. Massachusetts Medical Society; 2012 May 9;366(19):1759–1769.

44. Celgene. FDA expands indication for Revlimid® (lenalidomide) in combination with dexamethasone to include patients newly diagnosed with multiple myeloma [Internet]. ir.celgene.com. [cited 1991 Jun 2]. Available from: http://ir.celgene.com/releasedetail.cfm?releaseid=896912

45. Hofmann W-K, Koeffler HP. Myelodysplastic syndrome. Annu Rev Med. 2005;56(1):1–16. PMID: 15660498

46. Raza A, Meyer P, Dutt D, Zorat F, Lisak L, Nascimben F, Randt du M, Kaspar C, Goldberg C, Loew J, Dar S, Gezer S, Venugopal P, Zeldis J. Thalidomide produces transfusion independence in long-standing refractory anemias of patients with myelodysplastic syndromes. Blood. American Society of Hematology; 2001 Aug 15;98(4):958–965. PMID: 11493439

47. List A, Kurtin S, Roe DJ, Buresh A, Mahadevan D, Fuchs D, Rimsza L, Heaton R, Knight R, Zeldis JB. Efficacy of lenalidomide in myelodysplastic syndromes. N Engl J Med. Massachusetts Medical Society; 2009 Oct 8;352(6):549–557. PMID: 15703420

48. Raza A, Reeves JA, Feldman EJ, Dewald GW, Bennett JM, Deeg HJ, Dreisbach L, Schiffer CA, Stone RM, Greenberg PL, Curtin PT, Klimek VM, Shammo JM, Thomas D, Knight RD, Schmidt M, Wride K, Zeldis JB, List AF. Phase 2 study of lenalidomide in transfusion-dependent, low-risk, and intermediate-1–risk myelodysplastic syndromes with karyotypes other than deletion 5q. Blood. American Society of Hematology; 2008 Jan 1;111(1):86–93. PMID: 17893227

49. Adès L, Boehrer S, Prebet T, Beyne-Rauzy O, Legros L, Ravoet C, Dreyfus F, Stamatoullas A, Chaury MP, Delaunay J, Laurent G, Vey N, Burcheri S, Mbida R-M, Hoarau N, Gardin C, Fenaux P. Efficacy and safety of lenalidomide in intermediate-2 or high-risk myelodysplastic syndromes with 5q deletion: results of a phase 2 study. Blood. American Society of Hematology; 2009 Apr 23;113(17):3947–3952. PMID: 18987358

50. Fenaux P, Giagounidis A, Selleslag D, Beyne-Rauzy O, Mufti G, Mittelman M, Muus P, Boekhorst te P, Sanz G, del Cañizo C, Guerci-Bresler A, Nilsson L, Platzbecker U, Lübbert M, Quesnel B, Cazzola M, Ganser A, Bowen D, Schlegelberger B, Aul C, Knight R, Francis J, Fu T, Hellström-Lindberg E, Group FTM-0LDS. A randomized phase 3 study of lenalidomide versus placebo in RBC transfusion-dependent patients with Low-/Intermediate-1-risk myelodysplastic syndromes with del5q. Blood. American Society of Hematology; 2011 Oct 6;118(14):3765–3776. PMID: 21753188

51. Hoffmann M, Kasserra C, Reyes J, Schafer P, Kosek J, Capone L, Parton A, Kim-Kang H, Surapaneni S, Kumar G. Absorption, metabolism and excretion of [14C]pomalidomide in humans following oral administration. Cancer Chemother Pharmacol. Springer-Verlag; 2013 Feb;71(2):489–501. PMCID: PMC3556473

52. Richardson PG, Siegel D, Baz R, Kelley SL, Munshi NC, Laubach J, Sullivan D, Alsina M, Schlossman R, Ghobrial IM, Doss D, Loughney N, McBride L, Bilotti E, Anand P, Nardelli L, Wear S, Larkins G, Chen M, Zaki MH, Jacques C, Anderson KC. Phase 1 study of pomalidomide MTD, safety, and efficacy in patients with refractory multiple myeloma who have received lenalidomide and bortezomib. Blood. American Society of Hematology; 2013 Mar 14;121(11):1961–1967. PMCID: PMC4123324

53. Lacy MQ, Kumar SK, LaPlant BR. Pomalidomide plus low-dose dexamethasone (pom/dex) in relapsed myeloma: long term follow up and factors predicting outcome in 345 patients. ASH Annual Meeting …. 2012.

54. Leleu X, Attal M, Arnulf B, Moreau P, Traulle C, Marit G, Mathiot C, Petillon MO, Macro M, Roussel M, Pegourie B, Kolb B, Stoppa AM, Hennache B, Bréchignac S, Meuleman N, Thielemans B, Garderet L, Royer B, Hulin C, Benboubker L, Decaux O, Escoffre-Barbe M, Michallet M, Caillot D, Fermand JP, Avet-Loiseau H, Facon T. Pomalidomide plus low-dose dexamethasone is active and well tolerated in bortezomib and lenalidomide–refractory multiple myeloma: Intergroupe Francophone du Myélome 2009-02. Blood. American Society of Hematology; 2013 Mar 14;121(11):1968–1975. PMID: 23319574

55. Miguel JS, Weisel K, Moreau P, Lacy M, Song K, Delforge M, Karlin L, Goldschmidt H, Banos A, Oriol A, Alegre A, Chen C, Cavo M, Garderet L, Ivanova V, Martinez-Lopez J, Belch A, Palumbo A, Schey S, Sonneveld P, Yu X, Sternas L, Jacques C, Zaki M, Dimopoulos M. Pomalidomide plus low-dose dexamethasone versus high-dose dexamethasone alone for patients with relapsed and refractory multiple myeloma (MM-003): a randomised, open-label, phase 3 trial. Lancet Oncology. 2013 Oct;14(11):1055–1066. PMID: 24007748

56. U.S. Food and Drug Administration. FDA approves Pomalyst for advanced multiple myeloma [Internet]. [cited 2016 Jun 2]. Available from: http://www.fda.gov/NewsEvents/Newsroom/PressAnnouncements/ucm338895.htm

57. Mitsiades N, Mitsiades CS, Poulaki V, Chauhan D, Richardson PG, Hideshima T, Munshi NC, Treon SP, Anderson KC. Apoptotic signaling induced by immunomodulatory thalidomide analogs in human multiple myeloma cells: therapeutic implications. Blood. 2002 Jun 15;99(12):4525–4530. PMID: 12036884

58. Gupta D, Treon SP, Shima Y, Hideshima T, Podar K, Tai YT, Lin B, Lentzsch S, Davies FE, Chauhan D, Schlossman RL, Richardson P, Ralph P, Wu L, Payvandi F, Muller G, Stirling DI, Anderson KC. Adherence of multiple myeloma cells to bone marrow stromal cells upregulates vascular endothelial growth factor secretion: therapeutic applications. Leukemia. 2001 Dec;15(12):1950–1961. PMID: 11753617

59. Davies FE, Raje N, Hideshima T, Lentzsch S, Young G, Tai YT, Lin B, Podar K, Gupta D, Chauhan D, Treon SP, Richardson PG, Schlossman RL, Morgan GJ, Muller GW, Stirling DI, Anderson KC. Thalidomide and immunomodulatory derivatives augment natural killer cell cytotoxicity in multiple myeloma. Blood. 2001 Jul 1;98(1):210–216. PMID: 11418482

60. Higgins JJ, Pucilowska J, Lombardi RQ, Rooney JP. A mutation in a novel ATP-dependent Lon protease gene in a kindred with mild mental retardation. Neurology. NIH Public Access; 2004 Nov 23;63(10):1927–1931. PMCID: PMC1201536

61. Ito T, Ando H, Suzuki T, Ogura T, Hotta K, Imamura Y, Yamaguchi Y, Handa H. Identification of a primary target of thalidomide teratogenicity. Science. American Association for the Advancement of Science; 2010 Mar 12;327(5971):1345–1350. PMID: 20223979

62. Lu G, Middleton RE, Sun H, Naniong M, Ott CJ, Mitsiades CS, Wong K-K, Bradner JE, Kaelin WG. The myeloma drug lenalidomide promotes the cereblon-dependent destruction of Ikaros proteins. Science. American Association for the Advancement of Science; 2014 Jan 17;343(6168):305–309. PMCID: PMC4070318

63. Krönke J, Udeshi ND, Narla A, Grauman P, Hurst SN, McConkey M, Svinkina T, Heckl D, Comer E, Li X, Ciarlo C, Hartman E, Munshi N, Schenone M, Schreiber SL, Carr SA, Ebert BL. Lenalidomide causes selective degradation of IKZF1 and IKZF3 in multiple myeloma cells. Science. 2014 Jan 17;343(6168):301–305. PMCID: PMC4077049

64. Molnár A, Georgopoulos K. The Ikaros gene encodes a family of functionally diverse zinc finger DNA-binding proteins. Mol Cell Biol. American Society for Microbiology (ASM); 1994 Dec;14(12):8292–8303. PMCID: PMC359368

65. Cortes M, Wong E, Koipally J, Georgopoulos K. Control of lymphocyte development by the Ikaros gene family. Curr Opin Immunol. 1999 Apr;11(2):167–171. PMID: 10322160

66. Krönke J, Fink EC, Hollenbach PW, MacBeth KJ, Hurst SN, Udeshi ND, Chamberlain PP, Mani DR, Man HW, Gandhi AK, Svinkina T, Schneider RK, McConkey M, Järås M, Griffiths E, Wetzler M, Bullinger L, Cathers BE, Carr SA, Chopra R, Ebert BL. Lenalidomide induces ubiquitination and degradation of CK1α in del(5q) MDS. Nature. 2015 Jul 9;523(7559):183–188. PMCID: PMC4853910

67. Peters JM, McKay RM, McKay JP, Graff JM. Casein kinase I transduces Wnt signals. Nature. Nature Publishing Group; 1999 Sep 23;401(6751):345–350. PMID: 10517632

68. Wu S, Chen L, Becker A, Schonbrunn E, Chen J. Casein kinase 1α regulates an MDMX intramolecular interaction to stimulate p53 binding. Mol Cell Biol. American Society for Microbiology; 2012 Dec;32(23):4821–4832. PMCID: PMC3497597

69. Huart A-S, MacLaine NJ, Meek DW, Hupp TR. CK1alpha plays a central role in mediating MDM2 control of p53 and E2F-1 protein stability. J Biol Chem. American Society for Biochemistry and Molecular Biology; 2009 Nov 20;284(47):32384–32394. PMCID: PMC2781653

70. Schneider RK, Ademà V, Heckl D, Järås M, Mallo M, Lord AM, Chu LP, McConkey ME, Kramann R, Mullally A, Bejar R, Solé F, Ebert BL. Role of casein kinase 1A1 in the biology and targeted therapy of del(5q) MDS. Cancer Cell. 2014 Oct 13;26(4):509–520. PMCID: PMC4199102

71. Järås M, Miller PG, Chu LP, Puram RV, Fink EC, Schneider RK, Al-Shahrour F, Peña P, Breyfogle LJ, Hartwell KA, McConkey ME, Cowley GS, Root DE, Kharas MG, Mullally A, Ebert BL. Csnk1a1 inhibition has p53-dependent therapeutic efficacy in acute myeloid leukemia. J Exp Med. Rockefeller Univ Press; 2014 Apr 7;211(4):605–612. PMCID: PMC3978274

72. Fischer ES, Böhm K, Lydeard JR, Yang H, Stadler MB, Cavadini S, Nagel J, Serluca F, Acker V, Lingaraju GM, Tichkule RB, Schebesta M, Forrester WC, Schirle M, Hassiepen U, Ottl J, Hild M, Beckwith REJ, Harper JW, Jenkins JL, Thomä NH. Structure of the DDB1-CRBN E3 ubiquitin ligase in complex with thalidomide. Nature. 2014 Aug 7;512(7512):49–53. PMCID: PMC4423819

73. Chamberlain PP, Lopez-Girona A, Miller K, Carmel G, Pagarigan B, Chie-Leon B, Rychak E, Corral LG, Ren YJ, Wang M, Riley M, Delker SL, Ito T, Ando H, Mori T, Hirano Y, Handa H, Hakoshima T, Daniel TO, Cathers BE. Structure of the human Cereblon-DDB1-lenalidomide complex reveals basis for responsiveness to thalidomide analogs. Nat Struct Mol Biol. Nature Publishing Group; 2014 Sep;21(9):803–809. PMID: 25108355

74. Petzold G, Fischer ES, Thomä NH. Structural basis of lenalidomide-induced CK1α degradation by the CRL4CRBN ubiquitin ligase. Nature. Nature Publishing Group; 2016 Apr 6;532(7597):127–130. PMID: 26909574

75. Frei E. Gene deletion: a new target for cancer chemotherapy. Lancet. 1993 Sep 11;342(8872):662–664. PMID: 8103151

76. Nijhawan D, Zack TI, Ren Y, Strickland MR, Lamothe R, Schumacher SE, Tsherniak A, Besche HC, Rosenbluh J, Shehata S, Cowley GS, Weir BA, Goldberg AL, Mesirov JP, Root DE, Bhatia SN, Beroukhim R, Hahn WC. Cancer vulnerabilities unveiled by genomic loss. Cell. 2012 Aug 17;150(4):842–854. PMCID: PMC3429351

77. Ravid T, Hochstrasser M. Diversity of degradation signals in the ubiquitin-proteasome system. Nat Rev Mol Cell Biol. Nature Publishing Group; 2008 Sep;9(9):679–690. PMCID: PMC2606094

78. Sampaio EP, Sarno EN, Galilly R, Cohn ZA, Kaplan G. Thalidomide selectively inhibits tumor necrosis factor alpha production by stimulated human monocytes. J Exp Med. The Rockefeller University Press; 1991 Mar 1;173(3):699–703. PMCID: PMC2118820

79. Moreira AL, Sampaio EP, Zmuidzinas A, Frindt P, Smith KA, Kaplan G. Thalidomide exerts its inhibitory action on tumor necrosis factor alpha by enhancing mRNA degradation. J Exp Med. The Rockefeller University Press; 1993 Jun 1;177(6):1675–1680. PMCID: PMC2191046

80. Doench JG, Hartenian E, Graham DB, Tothova Z, Hegde M, Smith I, Sullender M, Ebert BL, Xavier RJ, Root DE. Rational design of highly active sgRNAs for CRISPR-Cas9-mediated gene inactivation. Nat Biotechnol. 2014 Dec;32(12):1262–1267. PMCID: PMC4262738

81. An J, Ponthier CM, Sack R, Seebacher J, Stadler MB, Donovan KA, Fischer ES. pSILAC mass spectrometry reveals ZFP91 as IMiD-dependent substrate of the CRL4CRBN ubiquitin ligase. Nat Commun. 2017 May 22;8:15398. PMCID: PMC5458144

82. Jin X, Jin HR, Jung HS, Lee SJ, Lee J-H, Lee JJ. An atypical E3 ligase zinc finger protein 91 stabilizes and activates NF-kappaB-inducing kinase via Lys63-linked ubiquitination. J Biol Chem. American Society for Biochemistry and Molecular Biology; 2010 Oct 1;285(40):30539–30547. PMCID: PMC2945548

83. Jin HR, Jin X, Lee JJ. Zinc-finger protein 91 plays a key role in LIGHT-induced activation of non-canonical NF-κB pathway. Biochem Biophys Res Commun. 2010 Oct 1;400(4):581–586. PMID: 20804734

84. Pikarsky E, Porat RM, Stein I, Abramovitch R, Amit S, Kasem S, Gutkovich-Pyest E, Urieli-Shoval S, Galun E, Ben-Neriah Y. NF-kappaB functions as a tumour promoter in inflammation-associated cancer. Nature. Nature Publishing Group; 2004 Sep 23;431(7007):461–466. PMID: 15329734

85. Ben-Neriah Y, Karin M. Inflammation meets cancer, with NF-κB as the matchmaker. Nat Immunol. Nature Publishing Group; 2011 Aug;12(8):715–723. PMID: 21772280

86. Harris PE, Ralph P, Gabrilove J, Welte K, Karmali R, Moore MA. Distinct differentiation-inducing activities of gamma-interferon and cytokine factors acting on the human promyelocytic leukemia cell line HL-60. Cancer Res. 1985 Jul;45(7):3090–3095. PMID: 2988760

87. Verdine GL, Walensky LD. The challenge of drugging undruggable targets in cancer: lessons learned from targeting BCL-2 family members. Clin Cancer Res. American Association for Cancer Research; 2007 Dec 15;13(24):7264–7270. PMID: 18094406

88. Hagner PR, Man HW, Fontanillo C, Wang M, Couto S, Breider M, Bjorklund C, Havens CG, Lu G, Rychak E, Raymon H, Narla RK, Barnes L, Khambatta G, Chiu H, Kosek J, Kang J, Amantangelo MD, Waldman M, Lopez-Girona A, Cai T, Pourdehnad M, Trotter M, Daniel TO, Schafer PH, Klippel A, Thakurta A, Chopra R, Gandhi AK. CC-122, a pleiotropic pathway modifier, mimics an interferon response and has antitumor activity in DLBCL. Blood. American Society of Hematology; 2015 Aug 6;126(6):779–789. PMCID: PMC4528065

89. Matyskiela ME, Lu G, Ito T, Pagarigan B, Lu C-C, Miller K, Fang W, Wang N-Y, Nguyen D, Houston J, Carmel G, Tran T, Riley M, Nosaka L, Lander GC, Gaidarova S, Xu S, Ruchelman AL, Handa H, Carmichael J, Daniel TO, Cathers BE, Lopez-Girona A, Chamberlain PP. A novel cereblon modulator recruits GSPT1 to the CRL4(CRBN) ubiquitin ligase. Nature. 2016 Jul 14;535(7611):252–257. PMID: 27338790

90. Kalliolias GD, Ivashkiv LB. TNF biology, pathogenic mechanisms and emerging therapeutic strategies. Nat Rev Rheumatol. 2016 Jan;12(1):49–62. PMCID: PMC4809675

91. Millrine D, Miyata H, Tei M, Dubey P, Nyati K, Nakahama T, Gemechu Y, Ripley B, Kishimoto T. Immunomodulatory drugs inhibit TLR4-induced type-1 interferon production independently of Cereblon via suppression of the TRIF/IRF3 pathway. Int Immunol. Oxford University Press; 2016 Jun;28(6):307–315. PMID: 26865412